Exploring the Mechanisms underpinning the Increased anti-Cancer Efficacy of Apaziquone in Hypoxic *in vitro* Breast Cancer

Laura Caroline Smith

Submitted in accordance with the requirements for the degree of Master of Science by Research

Supervisor: Dr Owen Kavanagh

York St John University

School of Science, Technology, and Health

July 2026

The Laura Caroline Smith confirms that the work submitted is their own and that appropriate credit has been given where reference has been made to the work of others.

Acknowledgments:

This work is dedicated to my friends, Elizabeth Dawson and Marion Turner, whose strength, resilience, and courage in the face of breast cancer have been nothing short of inspiring. Their journey throughout treatment into remission is a testament to the power of hope and determination. I am endlessly grateful for their friendship and honoured to celebrate this milestone with them through this work. This dedication is a small tribute to the immense impact they continue to have on those who know and love and love them.

First and foremost, my sincere thanks go to Dr Owen Kavanagh and Dr Adam Odell, whose insight, and encouragement were invaluable. Their expertise and patience helped shape this thesis from its earliest stages to completion.

I would like to extend my heartfelt thanks to Dr Kate Herbert, whose role as postdoctoral researcher was instrumental in both scientific and emotional dimensions of this work. Her deep expertise, tireless dedication to research, and generous mentorship in the lab provided clarity and direction during complex phase of the project. Beyond her academic contributions, Dr Herbert offered unwavering emotional support, fostering a compassionate environment that made even the most challenging days manageable. Her presence was a source of strength and inspiration throughout this journey.

A special thank you goes to my horses, Piglet and Minnie, who were always there when I needed an ear. Their quiet companionship, early morning rides, and the simple joy of being with them offered a much-needed escape from the pressures of research. In their own way, they reminded me to breathe and stay grounded and keep moving forward.

I am profoundly grateful to my parents for their support, encouragement, and love throughout this journey. Their belief in me never faltered, even when I doubted myself. From the earliest days of my education to the final stages of this project, they have been my foundation offering comfort and the kind of quiet strength that only parents can give. This achievement is as much theirs as it is mine.

To my wonderful friends, thank you for being my cheerleaders, sounding boards, and occasional therapist throughout this journey. Your laughter late night chats, spontaneous distractions, and steady encouragement helped me stay balanced and sane. Whether it was riding out with me to clear my head or standing beside me in the lab during long, demanding hours, your companionship made the hard days lighter and the good days even better. I'm especially grateful to my friend Caitlin, whose unwavering support, shared laughter, and steady presence were a true lifetime. Her friendship has meant the world to me, and I

couldn’t have done this without her. Whether you understood the details of my work or just knew when I needed a break, your presence made this experience richer and far more bearable. I’m lucky to have you in my corner.

Abstract

Apaziquone (EO9) is an indolequinone bio reductive drug which relies on the cytosolic enzyme NQO1 for the activation. However, alternative findings suggest enhanced efficacy under hypoxic even when NQO1 expression is low. The aims of this study were to investigate alternative activation mechanisms of EO9 under hypoxic conditions. In *vitro* assays were conducted on BT474 and T47D under normoxic and hypoxic conditions, measuring cell viability, drug efficacy, ROS production and the influence of NQO1 on EO9 activation. Under hypoxia, EO9 exhibited a markedly increased cytotoxicity as the ED_{50} for T47D cell decreased by approximately 200-fold, while BT474 cells showed a 100-fold reduction. Notably, NQO1 activity was low in both cell lines, at 3.00 $x10^{-3}$ µmol/mg/min in T47D and 6.74 $x10^{-3}$ µmol/mg/min in BT474 cells, suggesting that EO9 activation under hypoxia may occur via alternative pathways such as ROS mediated mechanisms. These findings challenge the reliance on NQO1 for EO9 activation and support EO9's use in hypoxic tumours with low NQO1 expression.

Contents

Title page……..……..……..……..……1

Acknowledgments page……..…….……3

Abstract…….……..……...….5

Abbreviations……..……9

1.Introduction……...……..……10

1.1 Breast cancer…….……...10

1.2 EO9…….……10

1.2.1 Overview of EO9……10

1.2.2 Mechanism of Action of EO9……..…….……...……10

1.3 NQO1……..……..…...……11

1.3.2 Activation of NQO1…….……...……11

1.3.2 NQO1 in hypoxic environments……..…….……11

1.4 NQO1 inhibitors……..……..……..…12

1.4.1 Dicumarol…….……..…….……12

1.5 Hypoxic environments…….……..……..…12

1.6 Reactive Oxygen Species (ROS)…….……..……13

1.6.1 What are Reactive Oxygen Species…….……..……13

1.6.2 ROS Inhibitors……..……..……..……13

1.73D cell culture systems for evaluating EO9 activity ……..……..……..……13

2.Aims and Objectives.……..……..……14

3.Materials and methods……..……..……..……..…15

3.1 Cell culture……..……...……..…..……15

3.2 Survival assay……..……..…..……15

3.3 Measurement of NQO1 activity……..……...……..…..……16

3.4 Immunohistochemistry staining…..……..……..…..……17

3.5 Dicumarol Cytotoxicity Assay……..……..……..……..…….19

3.6 Combination treatment of Dicumarol and EO9 to determine the effects of inhibiting NQO1 on EO9 activation……..……..…..…..……..…..…..……19

3.7 Determination of Reactive Oxygen species (ROS) levels with the treatment of EO9……..……..…..…...……..…….....….20

3.8 Determination of ROS levels with the treatment of EO9 and inhibition of NQO1 using Dicumarol……..……..……...……..…....…….20

3.9 Determination of ROS levels with ROS inhibitor……..……..……20

3.10 Survival assay with treatment of EO9 and Butylated Hydroxytoluene..……21

3.11 The effects of spheroids on EO9 efficacy……..……..……...……...21

3.12 Western blot……..……...……..…22

3.13 Statistical analysis software……...……24

4. Results……..……...……25

4.1 Immunochemical Analysis of HIF-1α as a marker of hypoxia in Breast cancer Cell lines……..……..……..…….……...…….25

4.2 Cytotoxic effects of EO9 against Breast cancer cell lines……..…….…….26

4.3 EO9 mediated DNA Damage Signalling in Breast cancer Cell lines ….……27

4.4 NQO1 expression in breast cancer cells…….…….....….29

4.5 Measurement of NQO1 enzymatic activity in cancer cells……...……..….32

4.6 The effect of NQO1 inhibition on EO9 efficacy in breast cancer cell lines…33

4.7 Inhibition of NQO1 Using Dicumarol in Breast Cancer cell lines…….…..….34

4.8 Assessment of Cell viability following Butylated Hydroxytoluene treatment and its in ROS suppression……..…….…….....….37

4.9 EO9 suppresses growth and integrity of Breast cancer Spheroids following prolonged exposure to EO9……..……...…….40

5. Discussion……..……..…….43

5.1 Hypoxia induced modulation of EO9 activity…….…….....….43

5.2 Dissecting the Role of NQO1 in hypoxia Driven EO9 activity……....….45

5.3 Dicumarol as a selective inhibitor of NQO1: Chemosensitivity and functional impact on EO9 activation……..……..…….....….46

5.4 The impact of ROS inhibition on EO9-Induced Cytotoxicity…….....….48

5.5 EO9-Induced Cytotoxicity in 3D Tumour Spheroids..…….....….49

5.6 Future Works……..…….....……..50

5.7 Conclusion……..…….……..……..……51

6. Supplementary data……..60

Abbreviations:

Full Name	Abbreviation
2-(N-morpholino) ethanesulfonic acid	MES
3-(4,5-dimethylthiazol-2-yl)-2,5-diphenyltetrazoium bromide	MTT
4′,6-diamidino-2-phenylindole	DAPI
Apaziquone	EO9
Bicinchoninic acid	BCA
Bovine serum albumin	BSA
Butylated Hydroxytoluene	BHT
Deoxyribonucleic Acid	DNA
Dichlorophenolindophenol	DCPIP
Dimethyl sulfoxide	DMSO
Dithiothreitol	DTT
Dulbecco's Modified Eagles media	DMEM
Effective dose 50	ED_{50}
Gamma H2A histone family X	γH2AX
Hypoxia-inducible factor 1-alpha	HIF-1α
Infectious dose 50	ID_{50}
Inhibitory concentration 50%	IC_{50}
NAD(P)H dehydrogenase (quinone)	NQO1
Phosphate-buffered saline	PBS
Reactive Oxygen Species	ROS
Reduced nicotinamide adenine dinucleotide	NADH
Roswell Park Memorial Institute	RPMI media
Tris-buffered saline with Tween 20	TBST

1.Introduction

1.1 Breast cancer

Breast cancer remains one of the most challenging cancers to treat, with surgery often being the primary intervention. Secondary treatments such as radiotherapy and chemotherapy are commonly employed to reduce the risk of recurrence (Ahmad, Wu, Y. and Yang, W. 2013). Surgical removal of breast tumours is invasive, typically involves extended recovery periods, and has been linked to negative impacts on patients' mental health. Breast cancer also carries a high recurrence related mortality rate; in a study of 1528 patients, 1092 (71%) experienced early recurrence deaths (Pedersen et al. 2022). However, this risk can be significantly reduced through postoperative radiotherapy which has been shown to lower recurrence rates from 35% to 19.3% (Darby et al. 2011). These factors highlight breast cancer as a strong candidate for the development of innovative and less invasive treatment approaches.

1.2 EO9

1.2.1 Overview of EO9

Apaziquone (EO9) is an indolequinone bio reductive drug which relies on the cytosolic enzyme NQO1 for the activation (Phillips, R.M., Hendriks and Peters 2013). EO9 showed promise *in vitro* studies but encountered setbacks when used in clinical trials due to decreased efficacy and significant clearance of EO9 (Puri et al. 2006). The poor systemic bioavailability of EO9 is thought to be due to metabolism by the enzyme NADPH cytochrome P450 reductase in red blood cells inactivating EO9 before delivery to the site (Puri et al. 2006; Phillips, R.M., Hendriks and Peters 2013). Furthermore, EO9's efficacy has been seen to be increased in bladder cancer with intravesical delivery due to reduced systemic clearance of EO9 (Puri et al. 2006).

1.2.2 Mechanism of action of EO9

EO9 is a bio reductive alkylating agent which requires the 2-electron enzymatic reduction by NAD(P)H dehydrogenase (quinone) (NQO1) to its active metabolite (hydroquinone) to exert its cytotoxic effects by DNA damage (see Figure 1) (Choudry et al. 2001; Xiong et al. 2022). In normoxic conditions, this activation of EO9 is already established as NQO1 facilitates the reduction therefore causing EO9's efficacy in NQO1-rich tumours (Choudry et al. 2001). NQO1 plays a pivotal role in cellular defence against oxidative stress by acting as a

detoxifying agent helping to reduce free radicals and harmful quinones such as EO9 (Yuhan, Khaleghi Ghadiri and Gorji 2024).

Semiquinone, are formed by the 1-electron reduction of EO9. Semiquinones are unstable free radicals that readily react with molecular oxygen to produce superoxide anions and hydrogen peroxide (Ho Yan 2005). This process, known as quinone redox cycling, amplifies reactive oxygen species (ROS) levels within cells causing damage to DNA, proteins and lipids triggering apoptotic pathways (Garcia-Llorens, El Ouardi and Valls-Belles 2025). In contrast hydroquinone are the product of 2-electron reduction and are more stable and less reactive, making hydroquinone's less likely to initiate oxidative stress (Phillips, R.M., Hendriks and Peters 2013).

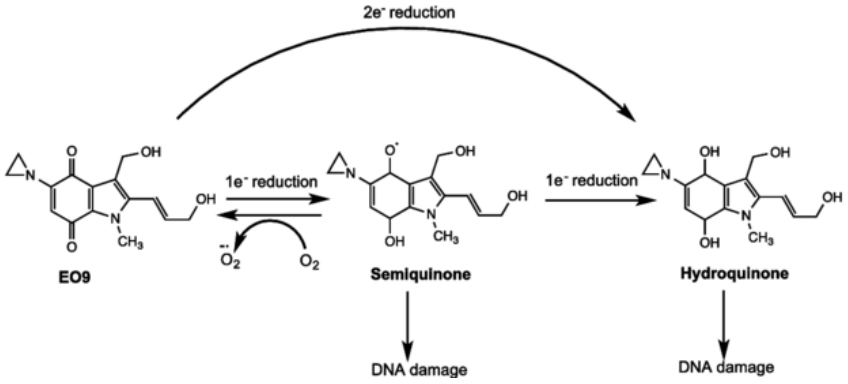

Figure 1: Activation of EO9 – *The reduction of EO9 to its active metabolites with a 1-electron reduction to semiquinone and 2-electron reduction to Hydroquinone facilitated by NQO1 (Phillips, R.M. 2016).*

1.3 NQO1

1.3.1 Activation of NQO1

NQO1 is a key enzyme responsible for the activation of EO9 and the expression of NQO1 relies on NRF2-KEAP1 signalling pathway, which is a cellular defence against oxidative stress (Hua et al. 2021; Weng et al. 2021). Under normoxic conditions, NRF2 is inactivated by a protein known as Keap1 but once the cell is exposed to cellular stress (e.g., ROS or toxins) causes the unbinding of NRF2 from Keap1 (Pant et al. 2023), where it then translocates to the nucleus activating the expression of NQO1 gene (Mutter, Park and Copple 2015; Shen, J. et al. 2017). Other factors such as aryl hydrocarbon receptor can also increase NQO1 levels in response to aryl hydrocarbon receptor it increases the cytotoxic effect of EO9 against tumour cells (Dong, H., Hao and Zhou, Z. 2021). This regulation of NQO1 helps cells respond to damage and plays an important role in the bio activation of EO9 (Choudry et al. 2001).

1.3.2 NQO1 in hypoxic environments

As previously mentioned, in normoxic conditions EO9 is converted by NQO1 to its cytotoxic active metabolite (hydroquinone). Although, in hypoxic conditions NQO1-rich tumours fail to show the same efficacy as in normoxia (Plumb and Workman 1994; Phillips, R.M. et al. 2006). While primarily activated by NQO1 under normoxic conditions, the efficacy of EO9 in hypoxic tumours is poorly understood highlighting a critical gap in knowledge regarding alternative reductive pathways and the contribution to bio activation of EO9 in low oxygen environments.

1.4 NQO1 inhibitors

1.4.1 Dicumarol

Dicumarol is a NQO1 inhibitor which is an enzyme responsible for the bio reduction of EO9 (Choudry et al. 2001). Dicumarol functions as a competitive inhibitor of NQO1 (IC_{50} 2.6nM) (Obi and Ezenwa 2018) and binds to NQO1 active site which prevents the 2-electron reduction of EO9 (Nolan et al. 2010). The IC50 (half-maximal inhibitory concentration) is the concentration of a substance needed to reduce a biological activity by 50% (Swinney 2011). This inhibition of NQO1 blocks the conversion of EO9 into its active metabolite hydroquinone which decreases enzyme activity (Choudry et al. 2001). Dicumarol has been widely used to validate the NQO1-driven activation of drugs in cancer cells (Johansson et al. 2003). Its ability to inhibit NQO1 activity has also made it a valuable tool for studying the role of this NQO1 in redox events and drug metabolism in tumour environments (Nolan et al. 2010; Aras et al. 2016)

1.5 Hypoxic environments

A hypoxic environment is one where the oxygen levels are significantly lower than normal with the failure of oxygenation of tissues but has no numerical value (Samuel and Franklin 2008). In a normal atmospheric environment oxygen makes up 20.9% of the atmospheric gas (Huppertz 2023; Bhutta, Alghoula and Berim 2024). Oxygen concentrations in tumours is typically much lower when compared to normal tissues, often falling to around 1.3% (Hompland, Fjeldbo and Lyng 2021). This occurs because tumours out-grow the blood supply and develop abnormal vasculature that hinders oxygen delivery (Liu, L. et al. 2025). In response to low oxygen, cells activate HIF-1α transcription factor which regulates genes involved in angiogenesis, metabolism, and survival (Liu, L. et al. 2025). HIF-1α promotes adaption to hypoxia by driving key hypoxic genes such as vascular endothelial growth factor, erythropoietin which enhances resistance to therapy, and drives angiogenesis and metastasis (Cheng, L. et al. 2017; Basheeruddin and Qausain 2024; Zhou, J. et al. 2024; Shaikat et al. 2025). Hypoxia also alters immune responses, making it a critical focus in cancer research and treatment strategies (Chen, Y. and Gaber 2021).

1.6 Reactive Oxygen Species (ROS)

1.6.1 What are Reactive Oxygen Species

ROS play a complex role in cellular physiology, acting as both signalling molecules and agents of damage depending on the concentration and context (Douda et al. 2015; Hu, Y. et al. 2024). At low to moderate levels, ROS contribute to essential processes such as cell proliferation, differentiation, and immune defence by controlling pathways such as MAPK, NRF2 (Son et al. 2011; Kasai et al. 2020). However, when ROS levels become excessive, it overwhelms the cell's antioxidant defences and induces oxidative stress (Hayes, J.D., Dinkova-Kostova and Tew 2020). High levels of ROS impair mitochondrial function, disrupts ATP production, and can trigger apoptosis and necrosis (Ježek, Cooper and Strich 2018). Thus, maintaining redox balance is vital for cellular health, and therapeutic strategies often aim to either control ROS levels or to exploit ROS' cytotoxic effects in cancer therapies (Glorieux et al. 2024).

1.6.2 ROS inhibitors

Butylated hydroxytoluene (BHT) is a synthetic antioxidant often used to inhibit ROS and prevent oxidative damage and stress in biological systems (Dawidowicz and Olszowy 2011). The mechanism of action involves donating hydrogen atoms to enable neutralisation of free radicals (Dawidowicz and Olszowy 2011). BHT is especially effective in protecting cellular lipids from oxidative degradation (Faraji et al. 2024). BHT has been seen to protect against hepatorenal toxicity caused by carbon tetrachloride which is a toxic chemical and has seen to decrease by ROS production by 17.69% (Dassarma et al. 2025). Although on the other hand BHT has shown to cause toxic effects in animal models with effects such as haemorrhage (Kahl 1992). But BHT abilities to modulate ROS makes it a useful compound for studying the effects of oxidative stress, but although due to its dual nature warrants careful application.

1.7 3D cell culture systems for evaluating EO9 activity

Traditionally 2D cell culture has been used to evaluate the effects of drugs such as EO9. A major limitation of 2D cell culture is that it does not mimic the tumour microenvironment. This can be overcome by the use of 3D cell culture which recreates this microenvironment to bridge the gap between clinical studies and *in vitro* studies due to being more representative of a tumour microenvironment. A spheroid is a type of 3D cell culture which self assembles into spherical clusters, which mimic the structure and behaviour of tumours (Białkowska et al. 2020).

Spheroids mimic the 3D microenvironment of solid tumours more accurately than monolayer cell culture. Spheroids exhibit gradients of oxygen, nutrients, and pH, leading to hypoxic cores and necrosis (Schaefer et al. n.d.; Zagaynova et al. 2017; Kirsh, Pascetta and Uniacke 2023). Spheroids develop dense architecture with tightly packed cells and the development of extra cellular matrix as spheroids mature which can be seen on day 7 (Piwocka et al. 2025). The extra cellular matrix is composed of collagen, fibronectin which can inhibit EO9 penetration into spheroids which makes solid tumours increasingly hard to treat (Bhattacharya et al. 2023).

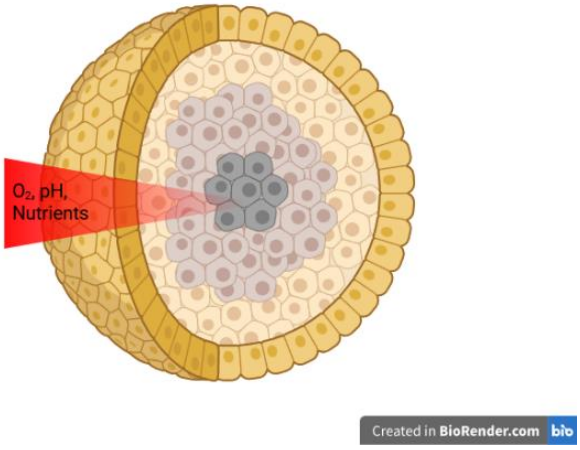

Figure 2: Oxygen gradient within a 3D spheroid – *A spheroid showing the oxygen gradients. The outer proliferative zone is well oxygenated while the intermediate layers exhibit reduced oxygen concentrations, transitioning into a hypoxic core at the centre. Colour intensity corresponds to oxygen concentration with warmer tones indicating higher oxygen concentration and cooler tones denoting hypoxia.*

1.8 Aims and Objectives

The aim of this study was to investigate the activation of mechanisms of EO9 under hypoxic conditions, particularly in breast cancer cell lines with low NQO1 expression. To achieve this, the following objectives were defined: (i) Evaluate EO9 cytotoxicity in BT474 and T47D breast cancer cell lines under normoxic and hypoxic conditions, (ii) Quantify NQO1 enzymatic activity in both cell lines and assess its relationship with EO9 efficacy, (iii) Measure ROS production as a potential alternative cytotoxic pathway for EO9 under hypoxia, and (iv) Finally, to determine whether EO9 activation and cytotoxicity can occur independently of NQO1 suggesting the involvement of alternative reductive mechanisms.

3. Materials and methods

3.1 Cell culture:

T47D is an oestrogen positive breast cancer cell line consisting of epithelial cells obtained via pleural effusion and presenting as infiltrating ductal carcinoma of the breast (ATCC no. HTB-133). The cells were grown in Dulbecco's Modified Eagles media (DMEM) media supplemented with 10% foetal bovine serum and 1% w/v Penicillin-Streptomycin.

BT474 (ATCC no. HTB-20) is derived from a solid invasive ductal carcinoma with epithelial morphology. It is oestrogen receptor positive and was obtained from a biopsy of a 60-year-old female. The cells were maintained in Roswell Park Memorial Institute media (RPMI media) supplemented with 10% foetal bovine serum and 1% w/v Penicillin-Streptomycin.

All cells were maintained as a monolayer in T75 and T25 flasks at 37°C in humidified atmosphere with 5% CO_2 under normoxic (21% O_2) or hypoxic conditions (1% O_2).

3.2 Survival assay

Preparation of EO9

Apaziquone (EO9) (Santa Cruz Biotechnology, catalogue number: sc-480043) was prepared by resuspending the lyophilised powder in sterile dimethyl sulfoxide (DMSO) to create a stock concentration of 10mM. Solubilised EO9 was aliquoted into Eppendorf tubes and stored at -20°C until required.

Seeding a 96 well plate

A T75 flask of adherent cells at 80-90% confluency was trypsinised to remove cells from the flask using TrypLE™ x1 Express Enzyme (catalogue number:12604021, Thermofisher Scientific). Cells were counted using a Cell Drop (DeNovix) and adjusted to $2x10^4$ cells per well before adhering overnight at 37°C on a 96-well plate (Sarstedt).

Treatment with EO9

To assess the cytotoxic effects of EO9 on BT474 and T47D cells, ten-fold dilutions (100,000-0.0001nM) of EO9 were prepared from 10 mM EO9 stocks.

Drug Exposure conditions

A 96 well plate was repeated in triplicate on three separate days and incubated with EO9 for 72-hours with EO9 between 100,000-0.0001nM at 37°C in corresponding O_2 levels.

MTT assay

To assess cell viability an MTT (3-(4,5-dimethylthiazol-2-yl)-2,5-diphenyltetrazoium bromide) cell survival assay was performed. MTT dissolved in phosphate-buffered saline (PBS) at a concentration of 5 mg/mL, was added to each well giving a final concentration of 500 µg/mL. Cells were incubated for 4 hours at 37°C to allow for the formation of formazan crystals. Following 4-hour incubation, media was removed and formazan crystals dissolved in DMSO. Absorbance was read using a Varioskan™ LUX multimode microplate reader at 540nM after shaking to ensure that all crystals were dissolved. Data was gathered in SkanIt 7.0 software in preparation for analysis in Excel to determine 50% effective dose (ED_{50}).

Calculating ED_{50}

Data was gathered in SkanIt 7.0 software in preparation for analysis in Excel to determine 50% effective dose (ED_{50}). The ED_{50} (effective dose 50%) is the dose of EO9 that produces 50% of its maximal effect. The ED_{50} was estimated using the linear interpolation formula ED_{50}= C +$\frac{a}{b}$ C, which relates the response difference and local slope to the dose producing 50% of the maximal effect. In this expression, a represents the difference between the observed response and the 50% response level, b is the gradient of the dose response relationship in this region, and C is the dose at which the initial response was measured.

3.3 Measurement of NQO1 activity

Preparation of cell cultures

Cells were removed from flasks as described above in Section 3.2 and $1x10^5$ cells were added to a T25 flask. Cells were allowed to reach late exponential growth phase (80% confluence).

Harvesting cells for NQO1 assay

Once late exponential growth phase was reached, the media was removed, and cells were extensively washed with PBS before adding 2mL of 0.25M sucrose. Cells were collected by scraping with a sterile cell scraper (Sarstedt) before transfer into a 25mL tube. The samples were placed on ice for 5 minutes to allow cooling prior to lysis by sonication (Qsonica Q55-220). Sonication was conducted at 20% amplification three times for 20 seconds each with 30 second intervals to release intracellular contents. Lysates were returned to ice to maintain the protein integrity.

Performing an NQO1 enzyme activity assay

The enzyme activity of NQO1 in each cell line was measured using reduced nicotinamide adenine dinucleotide (NADH) dependent reaction of dichlorophenolindophenol (DCPIP),

both in the presence and absence of dicumarol (NQO1 inhibitor). The difference in reduction rates reflects NQO1 enzymatic activity. Pre-chilled cell lysates were incubated for 1 hour in reaction buffer containing 50mM Tris buffer (pH 7.4), 6.23mM bovine serum albumin (BSA), and 2mM DCPIP. Samples containing 20μM of dicumarol were incubated for 1 hour to allow inhibition of NQO1. Following the 1-hour incubation. NADH was added to initiate the reaction with a final concentration of 200μM, initiating the reduction of DCPIP. Reactions were measured spectrophotometrically at 600nM over a 30 second (ΔA/min) period using a Jenway UV/Visible spectrophotometer. Dicumarol sensitive DCPIP reduction was determined by subtracting the ΔA/min value obtained in the presence of dicumarol from the ΔA/min in the absence of dicumarol.

Determination of protein concentration

Protein concentration was determined using Bicinchoninic acid (BCA) assay (Thermo Scientific™) according to the manufacturer's instructions. A working solution was created by mixing 50 parts of reagent A with 1 part regent B. Protein samples were pipetted into induvial wells of a 96-well plate, followed by the addition of BCA working regent at a 10:1 reagent to sample volume ratio. The assay was left to incubate for 30 minutes at 37°C and then read spectrophotometrically at 562 nm with a Jenway UV/Visible spectrophotometer. Cell lysate protein concentrations were determined from a standard curve of albumin (2,000mg/ml-25mg/ml) using linear regression.

Determination of NQO1 activity

The specific activity of NQO1 was calculated using the following formula:

Specific activity = ΔA/min / ε x P

Where ΔA/min is the dicumarol-sensitive rate of reduction of DCPIP, ε is the molar extinction coefficient for DCPIP (21 mM/cm), and P is the amount of protein in the cuvette in mg.

3.4 Immunohistochemistry staining

Seeding a 96 well plate

Cells were prepared as outlined in section 3.2.

Immunohistochemistry staining

For staining of γH2AX, cells grown on 96 well plates were treated with EO9 as outlined in section 3.4 for 24 hours.

Following incubation, media was removed from the wells, and cells washed 3 times with PBS before fixation using 4% paraformaldehyde for 15 minutes at room temperature. After fixation, cells were washed extensively with PBS. Cells were then permeabilised using a 0.5% Triton-X-100 for 10 minutes at room temperature, before further washing with PBS.

Cells were stained with primary antibody as stated in Table 1. Antibody dilutions were prepared in goat serum, and incubated on cells overnight at 4°C. After incubation, cells were washed with PBS before addition of secondary antibody (Table 1). To visualise cell nuclei, 300nM 4′,6-diamidino-2-phenylindole (DAPI) in goat serum was added to the sample for 2 hours at room temperature and then extensively washed with PBS.

Target	***Primary antibody***	***Primary antibody catalogue number and manufacturer***	***Primary antibody Dilution***	***Secondary Antibody***	***Secondary antibody catalogue number and manufacturer***	***Secondary antibody Dilution***
γH2AX	anti-H2A.X Phospho (Ser139) primary antibody	613401, BioLegend	1:1000	DyLight™ 488 Goat anti-mouse IgG (minimal x-reactivity)	405310 BioLegend	1:500
NQO1	anti-NQO1 primary antibody	NB200-209, Novusbio	1:1000	DyLight™ 488 Goat anti-mouse IgG (minimal x-reactivity)	405310 BioLegend	1:500
HIF-1α	HIF-1 alpha Antibody - BSA Free	NB100-479, Novusbio	1:1000	Goat anti-Rabbit IgG (H+L) Secondary Antibody [DyLight 633]	NBP1-76057, Bio-Techne	1:500

Table 1: *The primary and secondary antibodies combinations and dilutions used for Immunohistochemistry staining.*

Imaging and analysis

Once immuno-stained, the cells were imaged at 20X magnification under the EVOSFL2 microscope (Thermofisher Scientific) and images were saved for further analysis. The mean fluorescence of representative images was calculated using ImageJ (ImageJ 1.54p).

3.5 Dicumarol Cytotoxicity assay

Seeding a 96 well plate

Cells were prepared as outlined in section 3.2.

Treatment with dicumarol

Before NQO1 enzymatic activity could be assessed in *vitro*, the chemosensitivity of dicumarol on cell lines had to be assessed using the MTT assay (see above). Ten-fold (2mM-2nM) dilutions of dicumarol were prepared from a 10mM stock solution dissolved in DMSO containing NADH to aid solubility and incubated on the cells for 72-hours in corresponding O_2 conditions.

Cell survival assay

Cell survival was performed using an MTT assay as described in section 3.2. The results were analysed to determine the cytotoxic effects of dicumarol focusing on cell viability.

3.6 Combination treatment of Dicumarol and EO9 to determine the effects of inhibiting NQO1 on EO9 activation

Seeding a 96 well plate

Cells were prepared as outlined in section 3.2.

Treatment with Dicumarol and EO9

To determine the effects of cotreatment of EO9 and dicumarol on ROS production. Cells were treated with ten-fold dilutions of Dicumarol (2mM-2nM) (as described above). Cell were treated with the corresponding ED_{50} of EO9 calculated from section 3.2 (BT474 treated with 1.67μM and T47D with 0.02μM). Each plate was done in triplicate and incubated for 24-hours at 37°C in corresponding O_2 levels.

Cell survival assay

Cell survival was performed using an MTT assay as described above. The results were analysed to determine the cytotoxic effects of dicumarol in combination with EO9 focusing on cell viability.

3.7 Determination of Reactive Oxygen species (ROS) levels with the treatment of EO9

Seeding a 96 well plate

Cells were prepared as outlined in section 3.2.

Treatment with EO9

Cells were prepared as outlined in section 3.2.

ROS assay

H_2DCFDA is a fluorescent probe that detects ROS by becoming fluorescing upon oxidation. Media was removed from each of the wells and washed with PBS. In a dark room 30μM H_2DCFDA was added to each of the wells and incubated for 30 minutes at 37°C. Following incubation H_2DCFDA was removed from each of the wells and extensively washed with PBS. Following extensive washes PBS was left in each of the wells and plates were read using Varioskan™ LUX multimode microplate reader with an emission of 485nm and excitation 525nm and data was gathered in SkanIt 7.0 in preparation for analysis.

3.8 Determination of ROS levels with the treatment of EO9 and inhibition of NQO1 using Dicumarol

Seeding a 96 well plate

Cells were prepared as outlined in section 3.2.

Treatment with EO9 and Dicumarol

Ten-fold dilutions (0.2pM – 2mM) of dicumarol and EO9 (corresponding ED_{50} of EO9 from figure 4C) was added to the cells to create the final concentrations. Each plate was done in triplicate and incubated for 24-hours at 37°C in corresponding O_2 levels.

ROS assay

Cells were prepared as outlined in section 3.7.

3.9 Determination of ROS levels with ROS inhibitor

Seeding a 96 well plate

Cells were prepared as outlined in section 3.2.

Treatment of Butylated Hydroxytoluene

The effects of inhibition of ROS by butylated hydroxytoluene were assessed using a ROS assay to evaluate the effects of ROS inhibition. Ten-fold dilutions of butylated hydroxytoluene (50pM – 50 μM) dissolved in DMSO were prepared from a 1mM stock solution and diluted in DMEM to create final concentrations for each well. Each plate was done in triplicate and incubated for 24-hours at 37°C in corresponding O_2 levels.

ROS assay

Cells were prepared as outlined in section 3.7.

Calculating ID_{50}

Data was gathered in SkanIt 7.0 software in preparation for analysis in Excel to determine 50% inhibitory dose (ID_{50}). The ID_{50} (inhibitory dose 50%) is the dose of BHT that produces 50% inhibition. The ID_{50} was estimated using the linear interpolation formula ID_{50}= C +$\frac{a}{b}$ C, which relates the response difference and local slope to the dose producing 50% of the maximal effect. In this expression, a represents the difference between the observed response and the 50% response level, b is the gradient of the dose response relationship in this region, and C is the dose at which the initial response was measured.

3.10 Survival assay with treatment of EO9 and Butylated Hydroxytoluene

Seeding a 96 well plate

Cells were prepared as outlined in section 3.2.

Treatment of Butylated Hydroxytoluene

Ten-fold dilutions of Butylated Hydroxytoluene (with corresponding ID_{50} from figure 14C) dissolved in DMSO and were prepared from a 1mM stock solution and diluted in DMEM to create final concentrations for each well. Each plate was done in triplicate and incubated for 24-hours at 37°C in corresponding O_2 levels.

Treatment of EO9

Ten-fold dilutions of EO9 (0.01nM - 100μM) dissolved in DMSO were prepared from a 10mM stock solution and diluted in DMEM to create final concentrations for each well. Each plate was done in triplicate and incubated for 24-hours at 37°C in corresponding O_2 levels.

Cell survival assay

Cell survival was performed using an MTT assay as described in section 3.2.

3.11 EO9 efficacy in breast cancer cell spheroids

Development of spheroids

Spheroids were grown using low adherence plates (Starstedt Biofloat plates) and seeded at $5x10^5$ cells per well and left to incubate for 7 days at 37°C with media change on day 3.

Treatment of Spheroids with EO9

To observe the effects of EO9 on 3D cell culture spheroids were treated with EO9. Ten-fold dilutions of EO9 (1μM-100μM) were prepared from a 10mM stock solution to create the final concentration of EO9. Spheroids were allowed to incubate for 7 days.

Analysis of Spheroids

Plates were imaged under the EVOSFL2 microscope (Thermofisher Scientific) at days 1, 4, and 7 post treatment and were viewed under x4 magnification. Data was analysed post treatment by measuring diameter of the spheroids this was repeated in triplicate. Area of the spheroids were calculated, and representative images were shown in figure 16 below.

3.12 Western blot

Seeding a 6 well plate

A T75 flask of 80-90% confluency was trypinised to remove adherent from the flask and cell count was determined using cell drop (DeNovix). A 6 well plate was seeded with $9x10^5$ cells per well and allowed to adhere overnight. Each experiment was performed in triplicate and incubated for overnight to allow to adhere at 37°C in corresponding O_2 levels.

Preparation of samples

Media was removed from each of the wells and washed extensively with cold PBS to preserve protein integrity and minimise enzymatic degradation. Prewarmed SDS lysis buffer was added to each of the wells before lysates were transferred into an Eppendorf tube. Samples were boiled for 5 minutes at 95°C before sonication at 40% amplitude for 10 seconds to shear any DNA and release any undissolved proteins. Sample were then clarified by centrifugation for 10 minutes at 18000 x g and pellets discarded.

Determination of protein concentration

Protein concentrations of each cell lysate were determined by BCA assay as outlined in section 3.3.

Preparing samples for SDS-PAGE

A 4X SDS sample loading buffer (2% SDS, 10 mM Tris HCl pH 8.0, 1mM sodium orthovanadate) was prepared with dithiothreitol (DTT) as a reducing agent with a final

concentration of 100mM. Loading buffer was added to each sample at a 1X final concentration and samples mixed thoroughly. To denature and reduce proteins, samples were heated to 95°C for 10 minutes before brief centrifugation prior to gel loading.

Separation of proteins by SDS-PAGE and Western blotting

An electrophoresis tank was setup containing NuPAGE Bis-Tris precast gel (4-20%) and filled with 2-(N-morpholino) ethanesulfonic acid (MES) running buffer. 15µL of sample was added to each of the wells and a Benchmark™ Pre-Stained Protein ladder was loaded to the gel. The samples were run at 120V and 300A for 40 minutes before Western blotting. Gels were removed from casing, and a sandwich was created with pre-soaked blotting paper and nitrocellulose paper in semi dry transfer buffer containing 48mM tris base, 39mM Glycine, 0.04% SDS and 15% menthol. The semi dry transfer was completed by transferring to the Power blotter (Thermofisher Scientific) for 60 minutes.

Immunodetection

The nitrocellulose membrane was removed from the sandwich and non-specific binding sites were blocked using 5% skimmed milk power in Tris-buffered saline containing 0.1% Tween20 (TBST) for 60 minutes on an orbital rocker ensuring all surfaces are covered. The membrane was washed in TBST for 10 minutes and the membrane incubated in primary antibody as stated in table 2. Antibodies were prepared in TBST containing 1% bovine serum albumin (BSA) and incubated with membranes overnight at 4°C. The primary antibody was discarded, and the membrane was washed 3 times in TBST for 10 minutes each wash before the membrane was incubated for an hour in anti-mouse HRP conjugated at a concentration of 1:20,000 in TBST with 1% BSA. The secondary antibody was then discarded, and the membrane washed 3 times in TBST for 10 minutes each before membrane development with SuperSignal™ West Dura Extended Duration Substrate as per the manufacturer's instructions. The membrane was placed under the iBright for visualising and determining density of the bands. The images were saved for analysis on the iBright analysis tool.

Target	*Primary antibody*	*Primary antibody catalogue number and manufacturer*	*Primary antibody Dilution*	*Secondary Antibody*	*Secondary antibody catalogue number and manufacturer*	*Secondary antibody Dilution*
NQO1	anti-NQO1 primary antibody	NB200-209, Novusbio	1:1000	Anti-mouse IgG, HRP-linked Antibody	7076 Cell Signaling Techology	1:20,000

Table 2: *The primary and secondary antibodies combinations and dilutions used for a Western Blot*

3.13 Statistical analysis software

Quantitative image analysis was performed using ImageJ (ImageJ 1.54p), where measurements as means fluorescence intensity were obtained and acquired microscopy images. or protein expression analysis, iBright imaging system (Thermo Fisher Scientific) was used to quantify Western blot band intensities which are normalised to loading controls (β-actin).

Statical analyses were conducted using Graphpad prism (version 10). Group differences were evaluated by either one-way ANOVA with appropriate post hoc test or unpaired two-tailed t-tests to assess significance between groups depending on experimental design. Normality and homogeneity of variance were confirmed prior to applying parametric tests. All graphs were generated in Graphpad.

Cell viability was calculated using a custom Cell Wizard template in Microsoft Excel, which calculated viability percentages relative to positive controls. All experiments were performed in triplicate and outliers were identified using GraphPad's built in outlier detection tools and excluded only when justified.

4.0 Results

4.1 Confirmation of hypoxia by immunochemical analysis of HIF-1α as a marker of hypoxia in breast cancer cell lines

To verify if breast cell lines (BT474 and T47D) responded to hypoxic conditions (1% O_2) by stabilising hypoxia-inducible factor 1-alpha (HIF1- α) (Chua et al. 2010). The cells were stained with the marker of hypoxia, HIF-1α and examined by immunofluorescence microscopy.

Both cell lines showed increased mean fluorescence in hypoxic conditions (see Figure 3). A 1.5-fold increase in mean fluorescence was observed in BT474 cells in hypoxic conditions compared to normoxic conditions (Figure 3B). There was an increase of just under 2-fold of mean fluorescence for T47D in hypoxic conditions compared to normoxic conditions. This increase in the hypoxic marker HIF-1α confirms that hypoxia was induced when cells were incubated under 1% oxygen conditions.

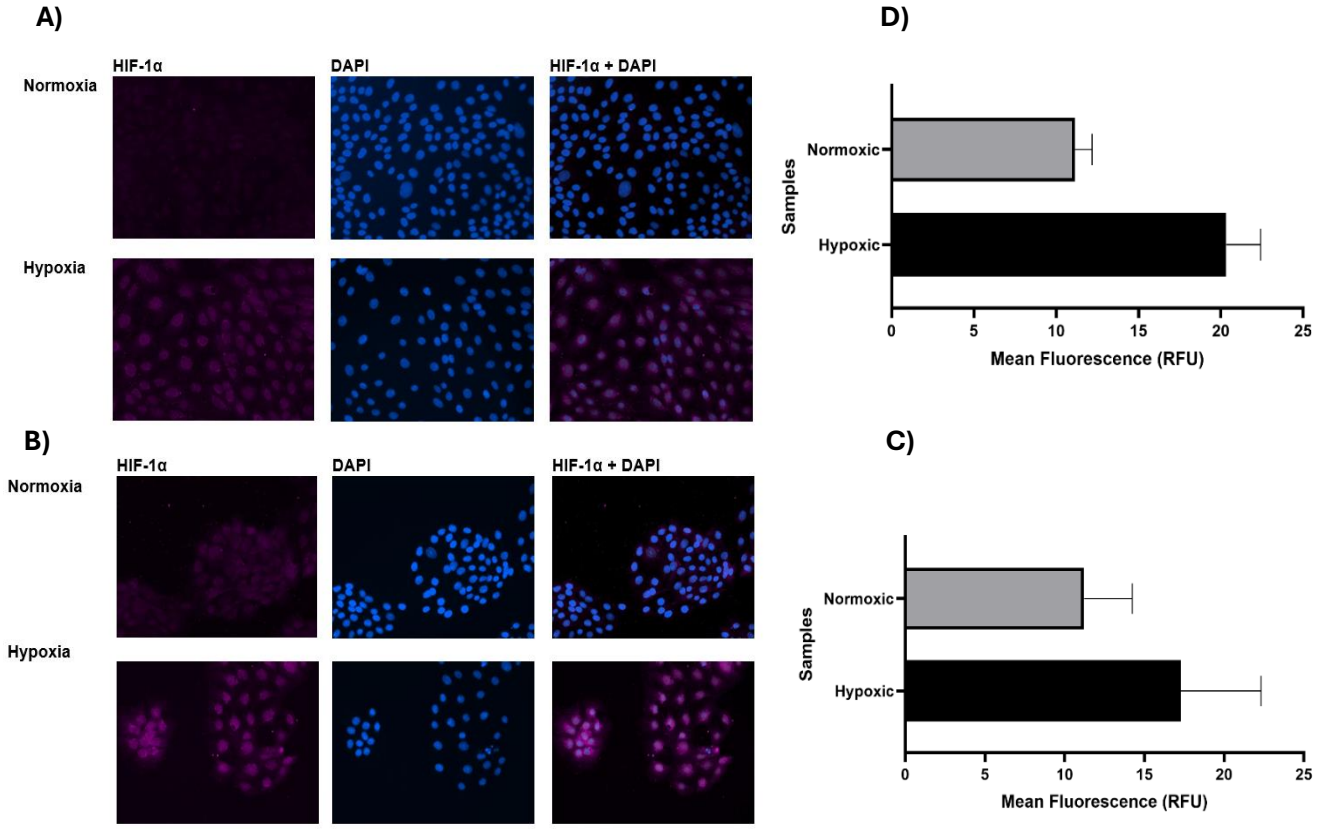

Figure 3: Confirmation of hypoxic conditions using* the *HIF-1α marker in Breast cancer cell lines. A-B) *A 96 well plate was seeded with* ***(A)*** *T47D or* ***(B)*** *BT474 cells at 2x10^4 cells per well and left to adhere overnight. Cells were then stained with HIF-1α and viewed under the EVOSFL2.* ***C-D) (C)*** *T47D and* ***(D)*** *BT474 representative images shown in figure 3A/B were analysed using ImageJ and mean fluorescence calculated and plotted with (+/- SD).*

4.2 Cytotoxic effects of EO9 against Breast cancer cell lines

To determine the cytotoxic effects of EO9 against Breast cancer cells BT474 and T47D lines were incubated with EO9 for 72 hours at the respective O_2 levels. The cytotoxic effects of EO9 were assessed using the MTT cell viability assay and an effective dose 50% (ED_{50}) was determined for each of the cell lines. ED_{50} represents the concentration of EO9 to achieve 50% cell death (Figure 4).

T47D was the most sensitive to the cytotoxic effects of EO9 in both hypoxic and normoxic conditions. T47D displayed an ED_{50} of 0.02μM in normoxic conditions but exhibited approximate 200-fold increase in potency under hypoxic conditions (ED_{50} = 0.0001μM.

On the other hand, BT474 showed decreased sensitivity to EO9 compared to T47D with a ED_{50} of 1.67μM in normoxia and a 100-fold increase in efficacy (ED_{50} 0.016μM) in hypoxic conditions. These results demonstrate that EO9 is effective against epithelial breast cancer cell lines but the potency increases markedly in hypoxic conditions.

A) **B)**

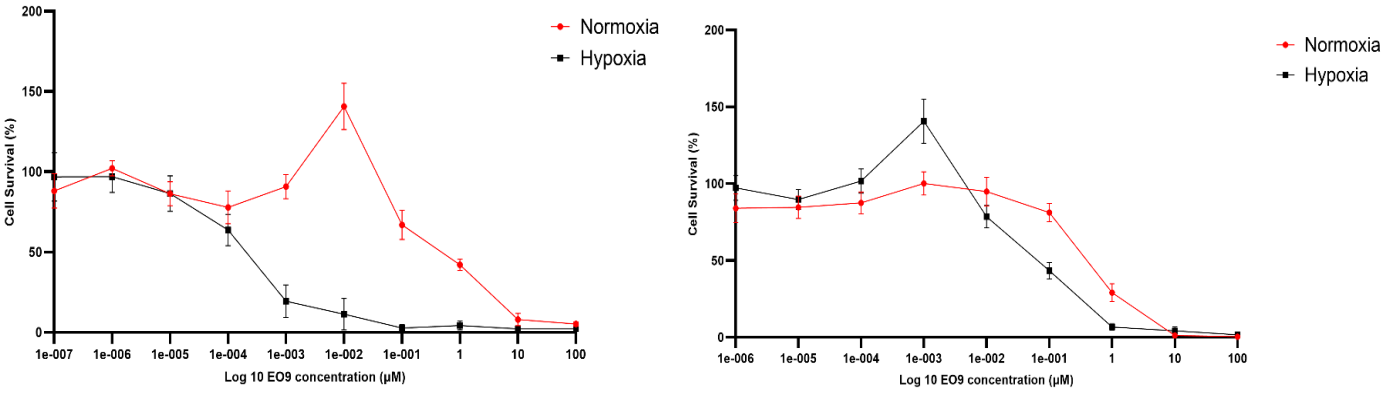

	T47D (μM)	**BT474 (μM)**
Hypoxia (21% Oxygen)	0.02 (-/+0.01)	1.67 (-/+0.7)
Normoxia (1% Oxygen)	0.0001 (-/+0.002)	0.016 (-/+0.05)
Hypoxic Cytotoxicity Ratio	200 (+/- 0.03)	104.38 (-/+ 0.01)

Figure 4: Cytotoxic effects of EO9 against Breast cancer cell lines over 72 hours. A-B) *A 96 well plate was seeded with* ***(A)*** *T47D or* ***(B)*** *BT474 at 2x10^4 cells per well and left to adhere overnight. The following morning cells were treated with 10-fold dilutions of EO9 (100,000-0.0001nM) for 72 hours and following incubation a cell survival assay was performed. All the cell survivals were relative to the untreated controls.* ***C)*** *The table shows the ED_{50} (+/- SD) of T47D and BT474 in hypoxia and normoxia calculated from figure 4A and 4B and the Hypoxic Cytotoxicity Ratio. Data expressed the mean of three independent experiments +/- SD.*

4.3 EO9 mediated DNA damage signalling in breast cancer cell lines

EO9 exerts its cytotoxic effect through creation of DNA breaks (Phillips, R.M. 2016). A marker of DNA damage (γ-H2AX) was used to determine the DNA damaging effects of EO9 against both BT474 and T47D breast cancer cell lines under hypoxia or normoxia. DNA damage was assessed by image analysis of Immunohistochemistry staining of γH2AX following EO9 incubation for 24 hours.

In T47D cells cultured in hypoxia, there was an increase in γH2AX staining observed at EO9 concentrations of 100pM, 10nM, and 1μM as seen in figures 5-7. Quantitative image analysis confirmed that staining intensity at concentrations 100pM, 10nM, and 1μM were significantly increased ($p < 0.01$) compared to normoxic controls (Figure 5 and 7A). In contrast, no significant changes in γH2AX staining were detected at 1pM or the untreated controls samples under hypoxic conditions. Normoxic staining across all concentrations showed minimal staining, consistent with baseline levels (Figure 5).

Immunohistochemical staining of BT474 cell under normoxic and hypoxic conditions revealed no changes in γH2AX staining across all concentrations (Figure 6 and 7). Quantitative analysis showed no significant differences between staining intensities between normoxia and hypoxia at 1pM, 100pM, 10nM, or 1μM, compared to the untreated controls. Doxorubicin treatment was used as a positive control.

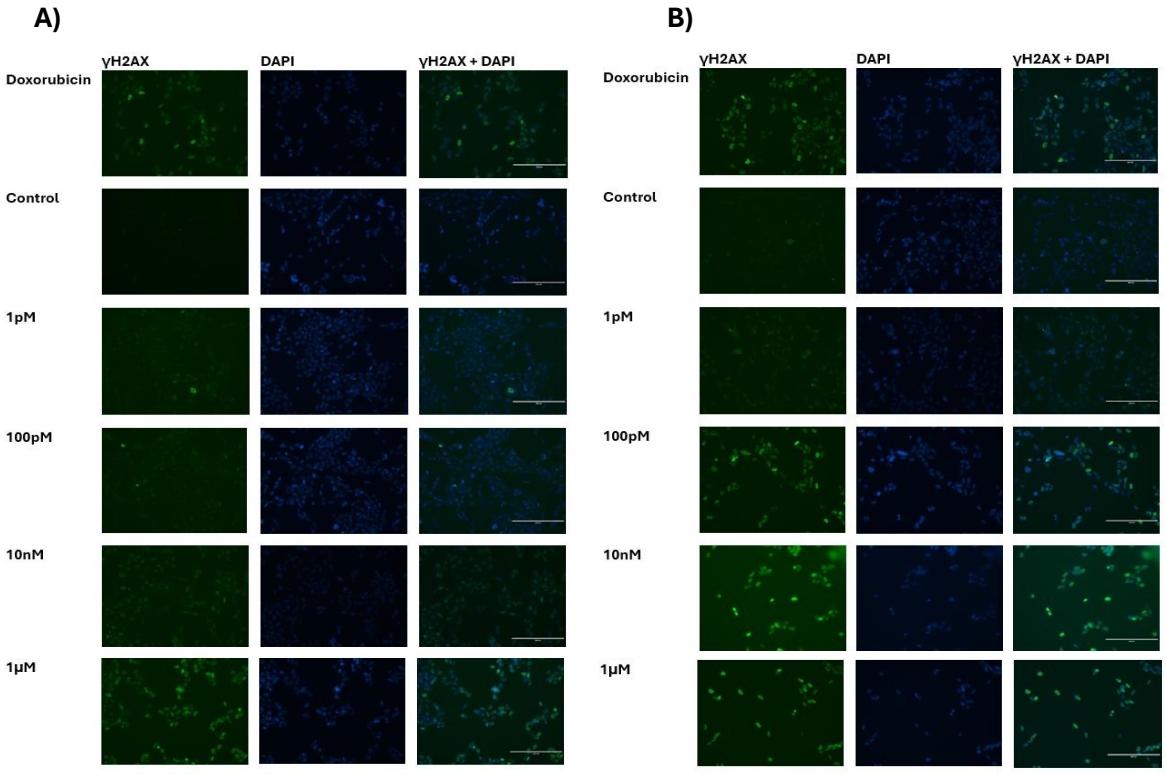

Figure 5. The effect of hypoxia with EO9 treatment for 72 hours on ɣH2Ax expression in T47D cells: A-B) *A 96 well plate was seeded with T47D (**A)** Normoxic (**B)** Hypoxic at 2x10^4 cells per well and left to adhere overnight and the following morning cells were stained with γ-H2AX. Images were viewed under the EVOS.*

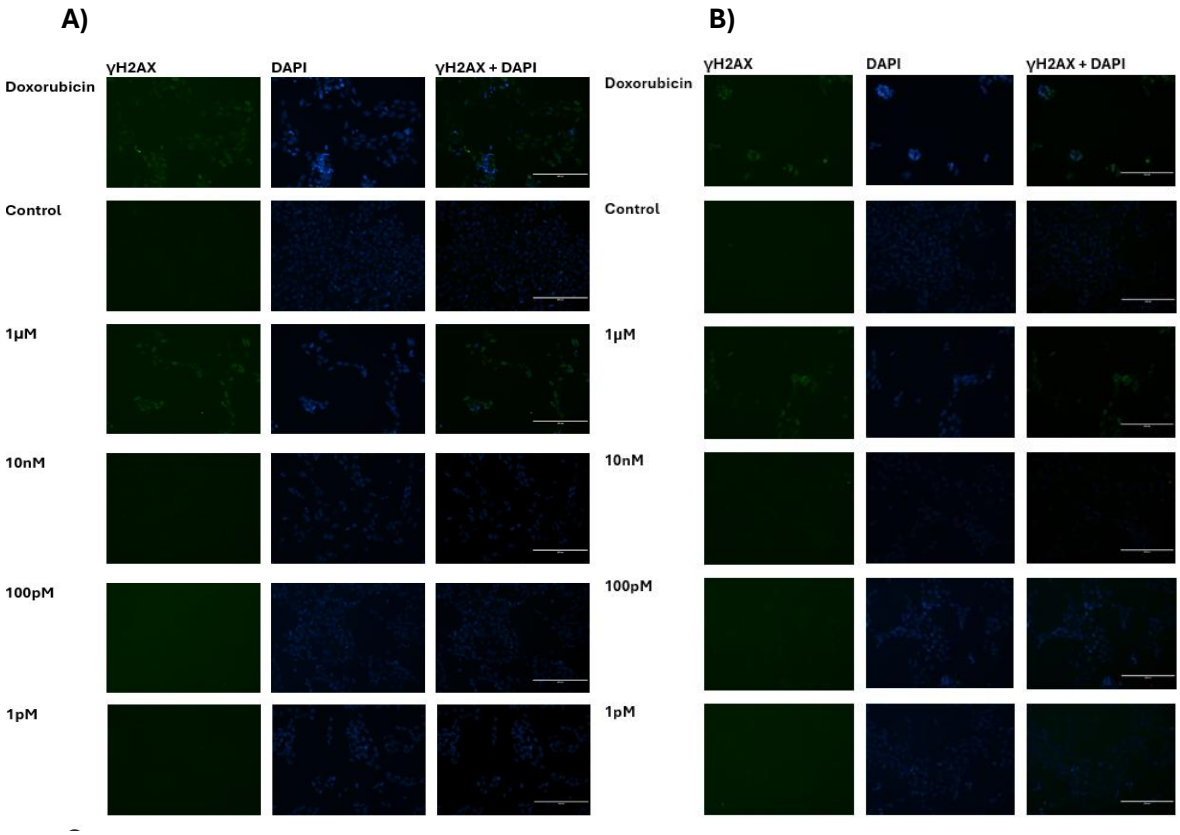

Figure 6. The effect of hypoxia with EO9 treatment for 72 hours on ɣH2Ax expression in BT474 cells. A-B) *A 96 well plate was seeded with BT474 (**A)** Normoxic (**B)** Hypoxic at 2x10^4 cells per well and left to adhere overnight and the following morning cells were stained with γ-H2AX. Images were viewed under the EVOS.*

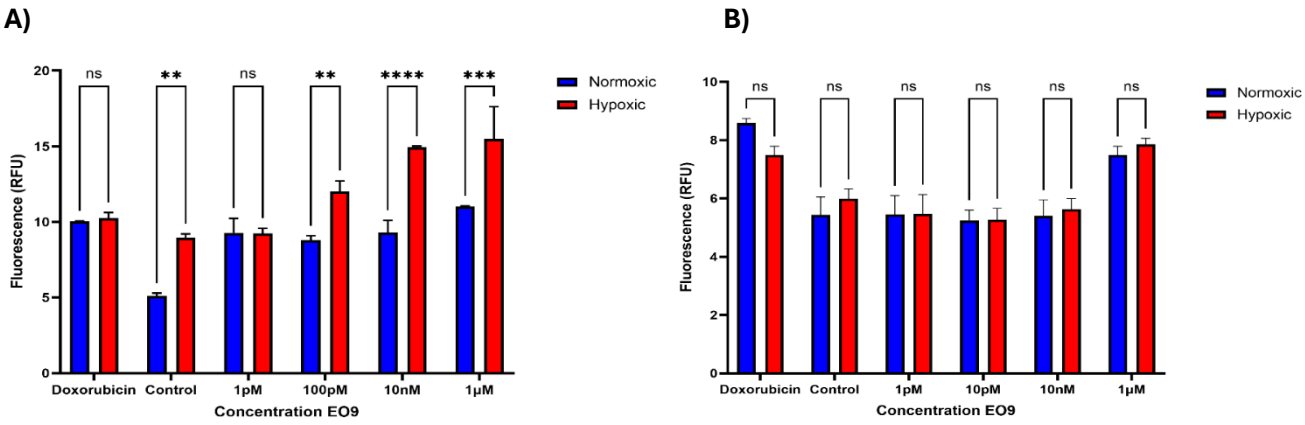

Figure 7. The effect of hypoxia and EO9 treatment on ɣH2Ax expression A-B) A) *T47D **B)** BT474 representative images shown in figure 5A+5B/6A+6B were analysed using imageJ and mean fluorescence calculated and plotted with (+/- SD).*

4.4 NQO1 expression in breast cancer cells

Levels of NQO1 expression were determined to see if there was a correlation with NQO1 levels and the efficacy of EO9. T47D and BT474 cells were stained using a NQO1 antibody and NQO1 levels assessed by calculating mean fluorescence in ImageJ to determine intracellular NQO1 levels. A Western blot was performed to quantify total NQO1 protein expression levels in BT474 and T47D cell lines, where β-actin was used as a housekeeping gene loading control.

Positive NQO1 immunocytochemical staining was detected in SiHa cells under normoxic conditions (Figure 8). The cervical cancer cell line, SiHa, is known to have high NQO1 expression levels (Ma, Y. et al. 2014) and was used as a positive control. This was confirmed by the strong cytoplasmic expression of NQO1 levels which is demonstrated with mean fluorescence of 13.03RFU (Figure 8). In contrast, CaSki cells, reported to express low NQO1 (Patiño-Morales et al. 2019) were used as a negative control (Patiño-Morales et al. 2019). As expected, CaSki cells displayed a significantly ($p < 0.0001$) decreased mean fluorescence NQO1 signal of 1.11RFU, validating the antibodies and assay. BT474 cells exhibited significantly ($p < 0.0001$) less cytoplasmic staining compared to SiHa with a mean fluorescence of 2.57. With T47D observed little cytoplasmic staining with a mean fluorescence of 2.00RFU. Both cell lines had comparable NQO1 expression levels and there was no significant difference between the cell lines.

NQO1 Immunocytochemical staining in hypoxia showed SiHa had strong cytoplasmic expression of NQO1 levels, demonstrated with mean fluorescence of 11.13RFU, which is comparable to normoxia. The negative control CaSki cell line, displayed a significantly ($p < 0.0001$) decreased mean fluorescence NQO1 signal of 1.22RFU. In hypoxic conditions BT474 cells mean fluorescence increased by 1.4-fold with a mean fluorescence of 3.611RFU and in T47D showed a slight decrease from 2.00RFU in normoxia to 1.90RFU in hypoxia which does not suggest a statistically significant difference (unpaired t-test $p > 0.05$).

Western blot analysis using an anti-NQO1 antibody revealed the expected band at 31kDa in all NQO1 positive cell lines indicating full length NQO1 is expressed. SiHa cells, showed strong staining at expected size 31kDa with a density of 18045AU which confirms high NQO1 expression. The negative control cell line, displayed no detectable NQO1 signal which validates the assay. Amongst the two breast cancer cell lines in normoxia, BT474 demonstrated moderate NQO1 expression with a density of 24377.5AU and T47D showed a 1.75-fold decreased expression of NQO1 levels compared to BT474 with a density of 13980AU (Figure 9).

In hypoxic conditions, NQO1 expression altered in both breast cancer cell lines, with BT474 cell NQO1 expression decreasing by over 3-fold with a density of 7760 in figure 9C. T47D expression also decreased in hypoxic conditions, where a 2-fold decrease was seen under hypoxic conditions with a density of 5916.5AU. β-actin was used as a housekeeping gene to ensure consistent loading and there was no significant difference between densities in all of the bands shown at 45kDa (figure 9C).

To determine whether hypoxia influences NQO1 expression, NQO1: β-actin ratios were quantified for all four cell lines under 1% and 21% oxygen. In SiHa cells, NOQ1 expression decreased under normoxia, significantly ($p<0.05$) increasing from 0.203 AU (+/- 0.01) at 1% oxygen to 0.290 AU (+/-0.05) at 21% oxygen, with a corresponding a 1.4-fold increase ($p<0.05$). BT474 cells showed a significant increase ($p<0.01$) from 0.079 AU (+/-0.03) at 1% oxygen to 0.390 AU (+/-0.02) at 21% oxygen, with a ~5-fold increase. CaSki cells exhibited low NQO1 expression in both conditions, with ratios of 1.433×10^{-9} AU in 1% oxygen and 1.243×10^{-9} AU at 21% oxygen, showing no significant difference between oxygen conditions ($p>0.05$) and confirming the status at a negative control. T47D cells demonstrated higher NQO1 expression under normoxia, significantly increasing ($p>0.05$) from 0.05 AU (+/- 0.06) at 1% oxygen to 0.20 AU (+/-0.09) at 21% oxygen.

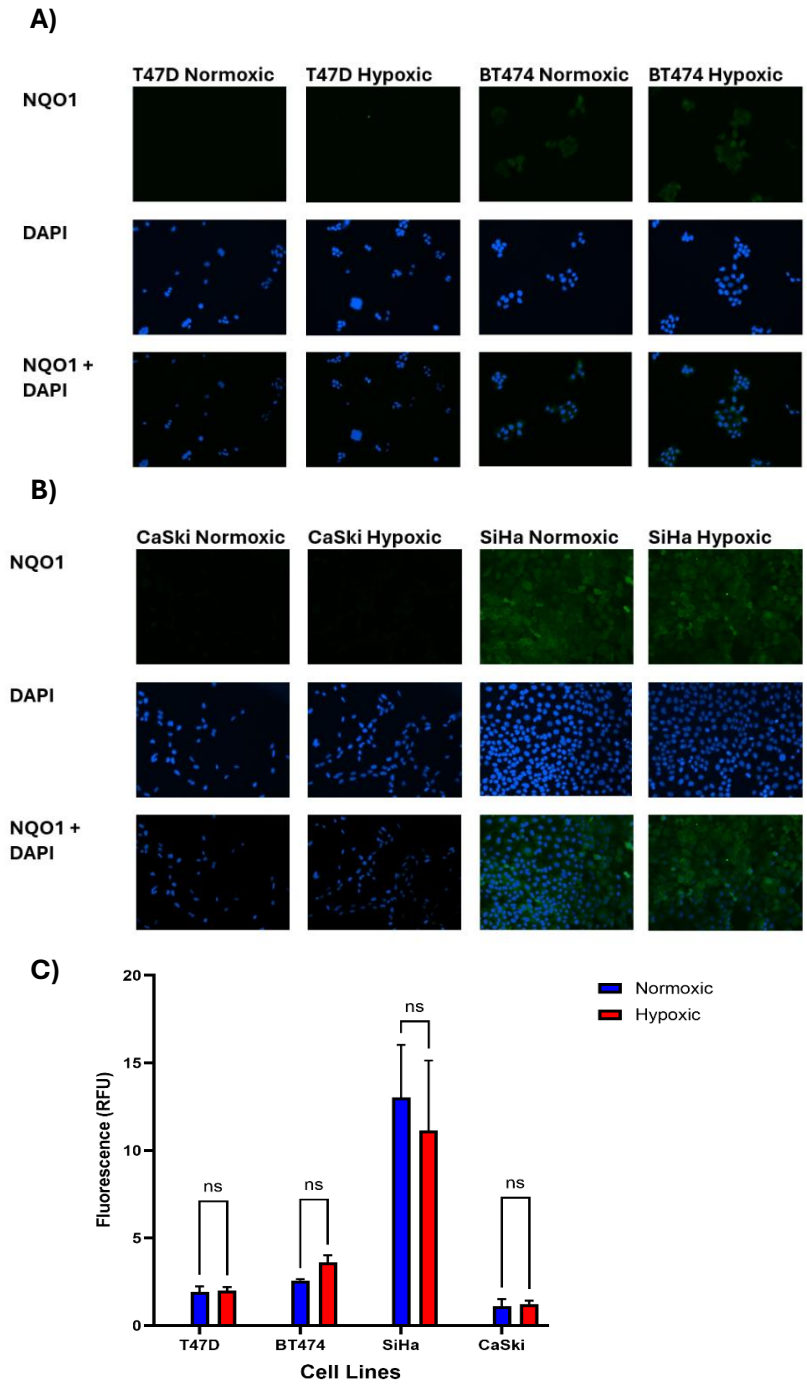

Figure 8: Detection of NQO1 in breast cancer cell lines – A-B) *A 96 well plate was seeded with* ***A)*** *T47D, BT474,* ***B)*** *CaSki and SiHa at 2x10^4 cells per well and left to adhere overnight in normoxic conditions and hypoxic conditions and the following morning cells were stained with NQO1. Images were viewed under the EVOS.* ***C)*** *Representative images shown in figure 8A+8B were analysed using imageJ and mean fluorescence calculated and plotted with (+/- SD).*

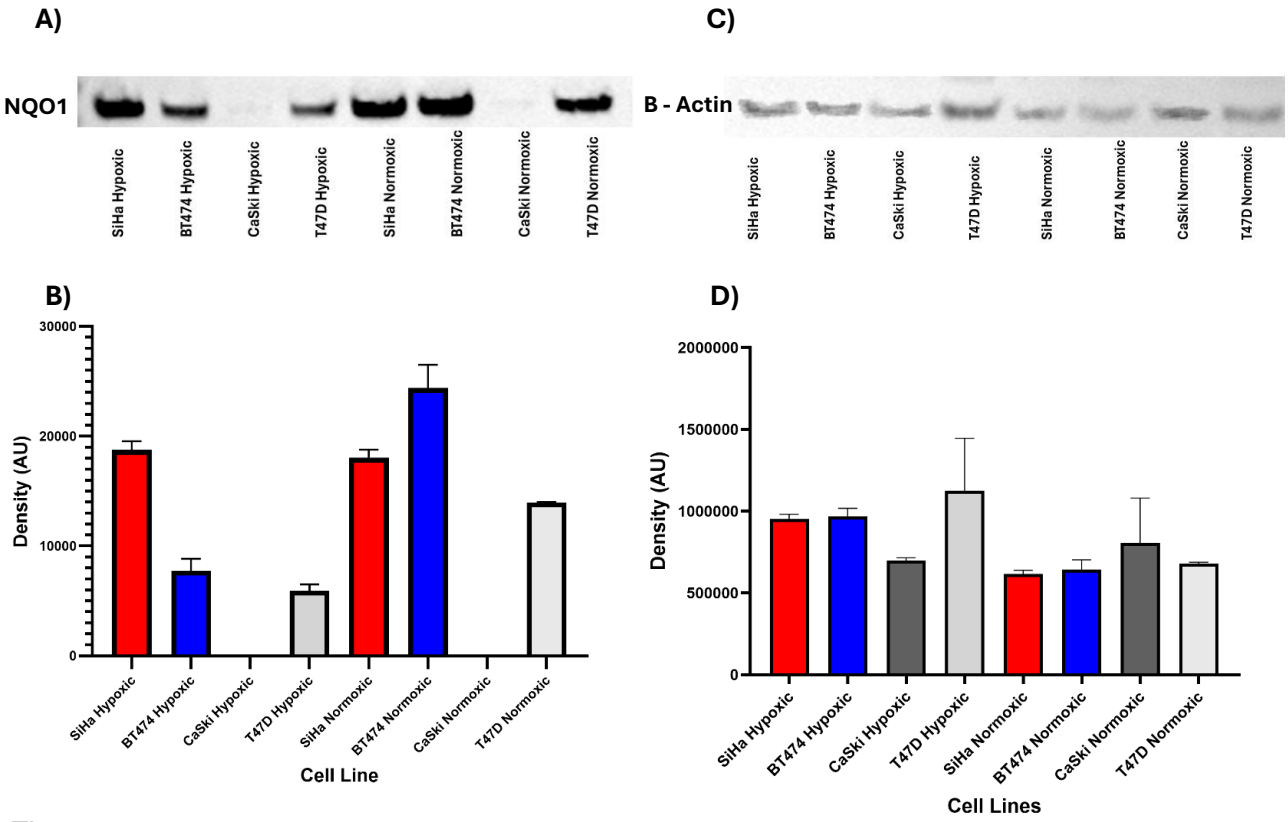

E)

	Hypoxia (1% Oxygen) (+/- SD)	**Normoxia (21% Oxygen) (+/- SD)**
	NQO1: β-Actin	**NQO1: β-Actin**
SiHa	0.20 (+/- 0.01)	0.30 (+/- 0.05)
BT474	0.08 (+/-0.03)	0.40 (+/- 0.02)
CaSki	1.433 x10^{-9} (+/-0.007)	1.243x10^{-9} (+/-0.002)
T47D	0.05 (+/- 0.06)	0.20 (+/- 0.09)

Figure 9: Detection of NQO1 in breast cancer cells via Western blot. A) *Western blot analysis of four cell lines. Protein lysates were from BT474, T47D, SiHa (positive control), and CaSki (negative control). Cell lines were subjected to SDS-page followed by immunoblotting with anti-NQO1 antibody.* ***B+D)*** *Representative images shown in* ***(B)*** *Figure 9A* ***(D)*** *Figure 9C were analysed using the iBright and density calculated and plotted with (+/- SD).* ***C)*** *Western blot analysis of four cell lines. Protein lysates were from BT474, T47D, SiHa, and CaSki. Cell lines were subjected to SDS-page followed by immunoblotting with β-actin antibody as housekeeping gene.* ***E)*** *Quantification of NQO1 expression normalised to β-actin. Densiometric ratios (NQO1: β-actin) were calculated from blots Figure 9A and Figure 9B and shown +/- SD.*

4.5 Measurement of NQO1 enzymatic activity in cancer cells

To determine levels of NQO1 enzyme activity, instead of protein expression levels. A spectrophotometric reduction of DCPIP in the presence and absence of dicumarol was conducted. The reduction in DCPIP directly relates to NQO1 activity, this change in absorbance was then used to calculate specific enzyme activity of NQO1 in all the cell lines.

SiHa cells exhibited the highest NQO1 enzymatic activity, consistent with high NQO1 expression observed below in figure 10. CaSki cells, the negative control, demonstrated low levels of NQO1 activity, validating the assay. T47D cells showed a specific enzyme activity of NQO1 of 3.00 $x10^{-3}$ µmol/mg/min which was 2-fold lower than NQO1 expression in BT474 with a NQO1 expression of 6.74 $x10^{-3}$ µmol/mg/min.

Cell Line:	**NQO1 Activity ($x10^{-3}$ µmol/mg/min)**
T47D	3.00 (+/- 0.02)
BT474	6.74 (+/- 0.04)
CaSki	$1.11x10^{-2}$ (+/- 0.001)
SiHa	18.31 (+/- 0.05)

Table 3: Dicumarol sensitive NQO1 activity assessed by DCPIP reduction: A) *T47D, BT474, CaSki, and SiHa, NQO1 activity levels assessed by the spectrophotometric reduction of DCPIP in the presence and absence of dicumarol.*

4.6 The effect of NQO1 inhibition on EO9 efficacy in breast cancer cell lines

To determine the direct cytotoxic effects of dicumarol and in combination with EO9 against BT474 and T47D breast cancer cell lines. Both cell lines were incubated with dicumarol and with combinations of EO9 and dicumarol for 72 hours in the respective O_2 levels. The cytotoxic effects were assessed using a cell viability assay and a ED_{50} was determined for each of the cell lines in normoxic conditions.

Prior to determining the influence of the NQO1 inhibitor (dicumarol) on EO9 induced cytotoxic activity, it was necessary to assess any direct cytotoxic effects of dicumarol on the BT474 and T47D. To determine the cytotoxicity of dicumarol a cell survival assay was performed on BT474 and T47D cells. T47D showed no significant decrease ($p < 0.05$) or increase in cell viability with incubation of dicumarol at concentrations of between 2000µM and 0.000002µM for 72 hours. BT474 showed no significant decrease ($p < 0.05$) or increase in cell viability with incubation of dicumarol at concentrations of 2000µM-0.000002µM for 72 hours. These results show that dicumarol is not directly cytotoxic to either cell lines and does not promote cell growth.

Next, combination treatments of dicumarol with EO9 were performed to determine the effects of inhibiting NQO1 on EO9 efficacy. T47D was treated with the corresponding ED_{50}

from figure 4C for 72 hours and cell viability assessed. A significant decrease ($p < 0.001$) in cell viability was seen in all concentrations compared to the original ED_{50} (Figure 11). BT474 was treated with the corresponding ED_{50} from figure 4C for 72 hours and cell viability assessed. BT474 cells showed a significant decrease ($p < 0.001$) in cell viability under all concentrations compared to the ED_{50} of EO9 alone, calculated from figure 4C.

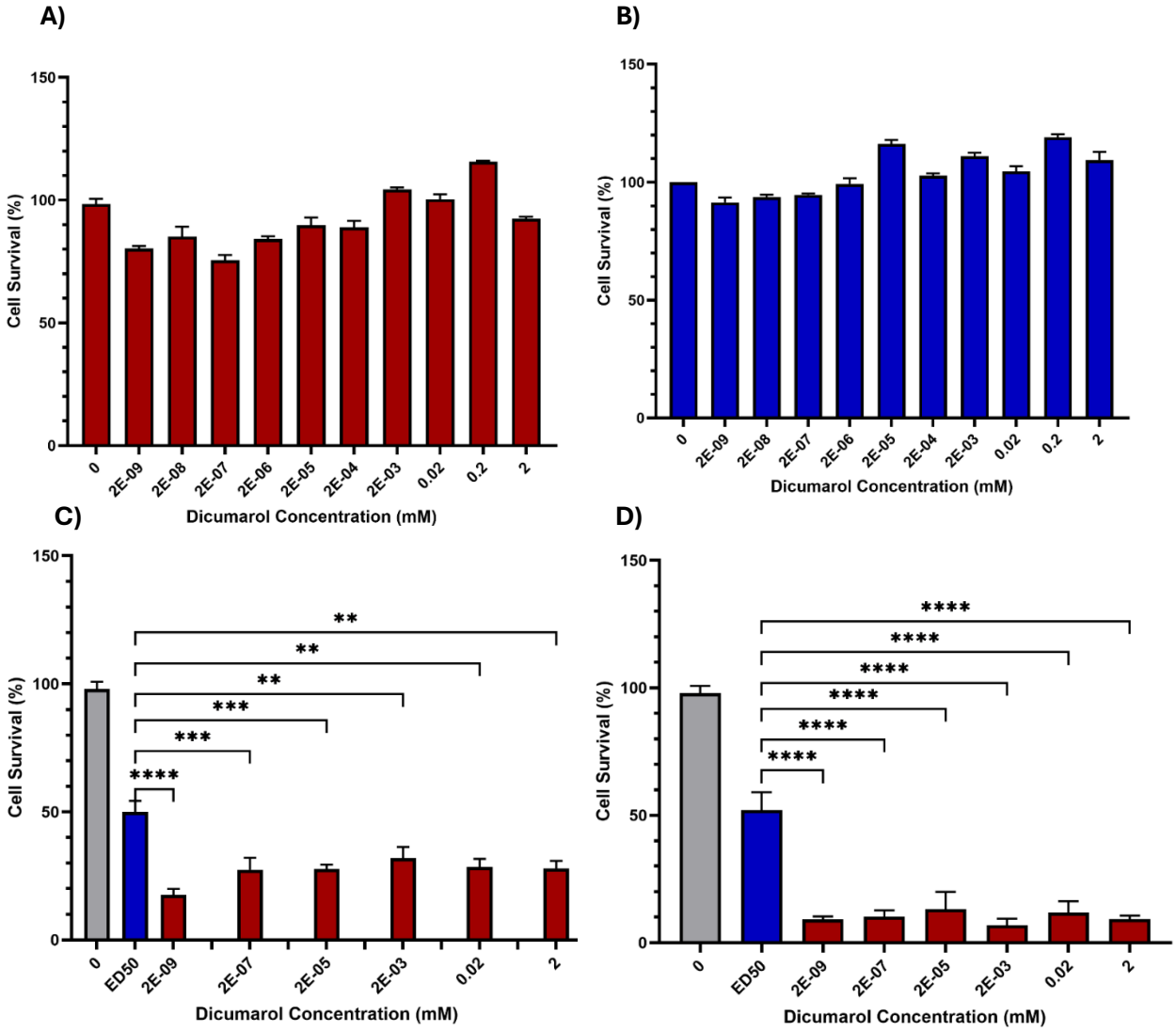

Figure 11: Cytotoxic effects of dicumarol and EO9 on breast cancer cell lines under Normoxic conditions. ***A-B)*** *The cytotoxic response of* ***(A)*** *T47D* ***(B)*** *BT474 following treatment with dicumarol for 72 hours, highlighting dose dependent effects on cell viability.* ***C-D)*** *The cytotoxic response of* ***(C)*** *T47D and* ***(D)*** *BT474 following co-treatment with dicumarol and corresponding ED_{50} for EO9 for 72 hours, demonstrating differential sensitivity and potential therapeutic implications.*

4.7 ROS production following inhibition of NQO1 using dicumarol in breast cancer cell lines

This section focuses on the impact of inhibiting NQO1 in BT474 and T47D, which were incubated with dicumarol and EO9 for 72, as well as with EO9 alone. To examine how inhibition of NQO1 affects the production of ROS in EO9 treated cells. In figure 12

fluorescence levels H_2DCFDA are measured in T47D and BT474 with treatment EO9 with concentrations ranging from 1pM to 1µM. T47D cells in normoxia, treatment with EO9 below 1nM significantly increased ROS levels compared to the control ($p < 0.001$). Specifically, 1pM of EO9 led to a 32% increase in ROS, reaching 3.6RFU, while 1nM resulted in a 22% increase to 3.0 RFU.

Under hypoxic conditions, EO9 treatment also elevated ROS levels at all concentrations compared to normoxia (figure 12A). The most significant increase was observed at concentrations above 1nM ($p < 0.001$), whereas 1pM showed a small but still significant increase in ROS ($p < 0.01$) (figure 12A).In BT474 cells under normoxic conditions, EO9 treatment significantly increased ROS production at all concentrations compared to the control ($p < 0.001$) (figure 12B). At 1pM, ROS levels rose by 28% relative to the control. Under hypoxic conditions, EO9 treatment in BT474 cells increased ROS across concentrations ranging from 1 pM to 1 µM (figure 12B). At 1M, ROS production was nearly twice as high as in the control group.

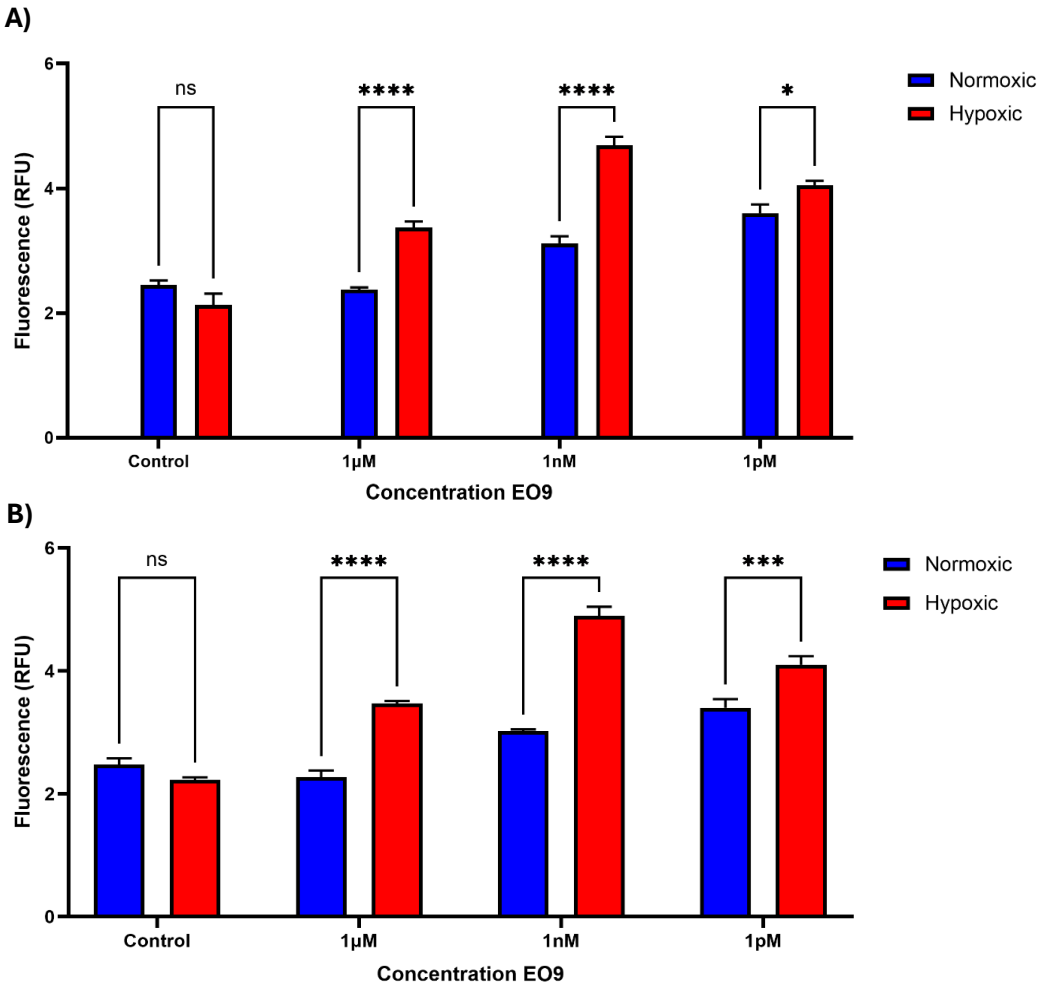

Figure 12: The effects of EO9 treatment with ROS production on breast cancer cell lines. A-B) (A)*T47D* ***(B)*** *BT474 cells were treated with EO9 (1μM – 1pM) for 72 hours. ROS levels on a 96-well plate were measured using emission of 485nm and excitation 525nm.*

Fluorescence levels of ROS were measured in T47D and BT474 with treatment EO9 and dicumarol (2mM to 2nM). T47D in normoxic conditions treatment with EO9 and dicumarol and just EO9 significantly increases ROS in all concentrations ($p < 0.001$) compared to the control. For T47D in hypoxic conditions, co-treatment with EO9 and dicumarol and treatment with EO9 alone, significantly increased (Figure 13) ($p < 0.05$) ROS at all concentrations tested compared to the control treatment and normoxic conditions. The greatest increase was observed at 2mM dicumarol in hypoxia, where a 3-fold increase in ROS production to 7.8RFU was seen compared to the control. BT474 saw a significant increase ($p < 0.05$) in ROS production in hypoxic conditions compared to normoxic conditions, with the greatest increase in ROS production evident at 2mM of dicumarol with over a 2-fold increase (16.6RFU) in ROS production in hypoxia.

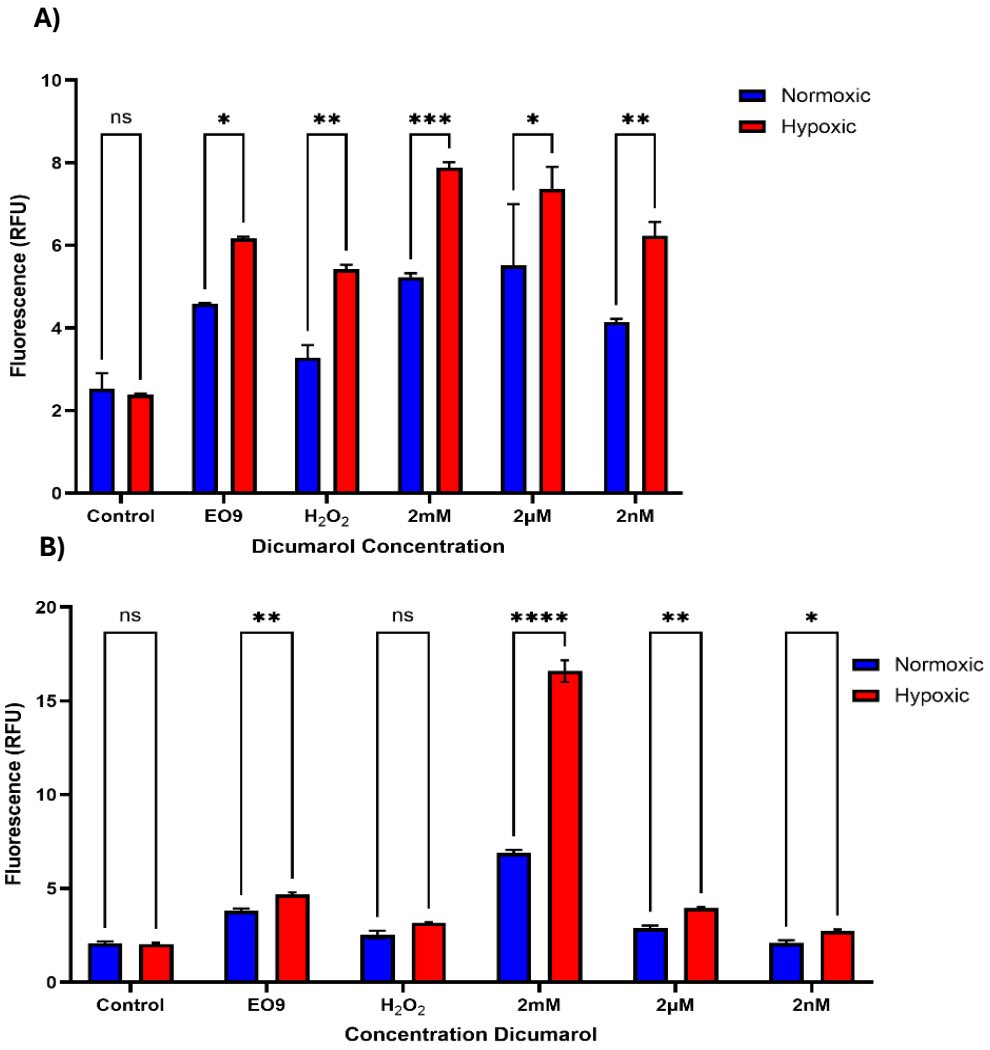

Figure 13: The effects of NQO1 inhibition on breast cancer cell lines. A-B) *(**A**)T47D **(B)** BT474 cells were treated with the corresponding $ED_{50\ of}$ EO9 and a range of dicumarol concentrations (2mM – 2nM) for 72 hours. ROS levels on a 96-well plate were measured using emission of 485nm and excitation 525nm.*

4.8 Assessment of cell viability following butylated hydroxytoluene treatment and its role in ROS suppression

To determine whether ROS mediates the enhanced efficacy of EO9 under hypoxic conditions, ROS production was inhibited with butylated hydroxytoluene (BHT). BT474 and T47D were treated with BHT in combination with EO9 for 72 hours in the respective O_2 levels. The effect of ROS suppression by BHT was assessed using a cell viability assay as described in section 3.6 to assess the effect of ROS inhibition on cell viability and to determine if ROS suppression alters the efficacy of EO9. An ED_{50} was determined for each of the conditions with the use of a cell wizard.

BT474 was the most sensitive to BHT under both normoxic and hypoxic conditions. BT474 shown an ID_{50} of 0.0794μM (+/- SD) in normoxic conditions but a 100-fold increase in ID_{50} of 7.6223μM (+/- SD) in hypoxic conditions. On the other hand, T47D was less sensitive BHT with an ID_{50} of 6.2682μM in normoxic conditions but decreased 2-fold in hypoxic Conditions with an ID_{50} 3.1498μM.

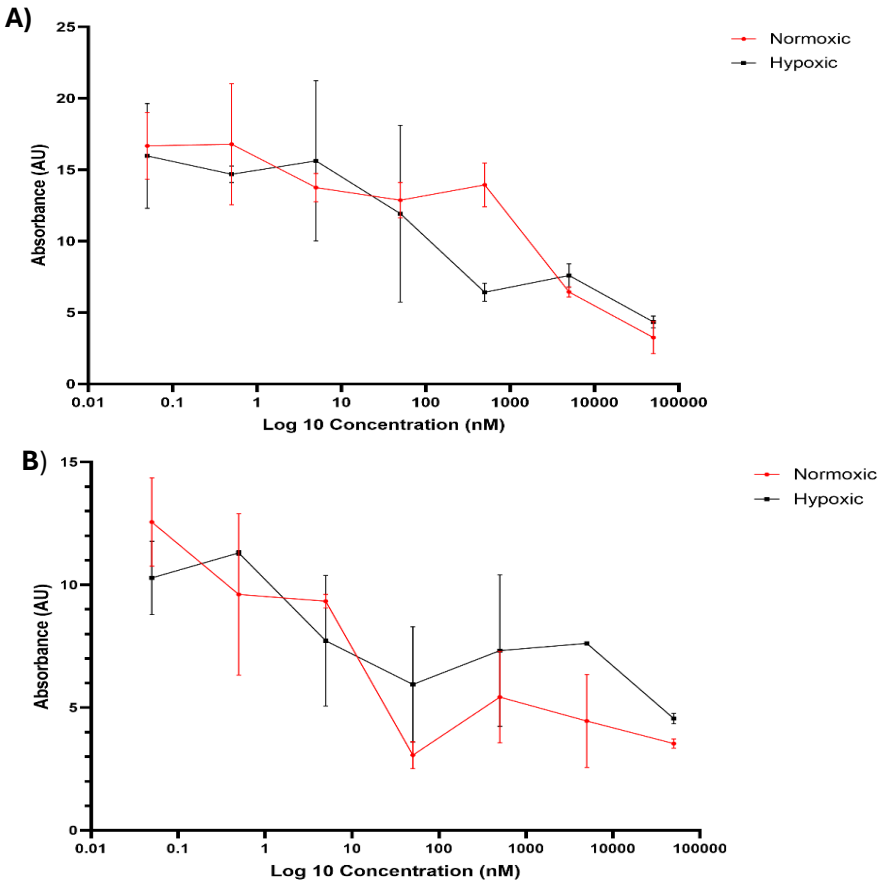

C)

	EO9		BHT	
	T47D (+/- SD) (µM)	**BT474 (+/- SD) (µM)**	**T47D (+/- SD) (µM)**	**BT474 (+/- SD) (µM)**
Normoxia (21% Oxygen)	*0.02 (-/+0.01)*	*1.67 (-/+0.7)*	6.2682 +/- 4.324	0.0794 +/- 0.003
Hypoxia (1% Oxygen)	*0.0001 (-/+0.002)*	*0.016 (-/+0.05)*	3.1498 +/-3.732	7.6223 +/- 1.844

Figure 14: The effect ROS suppression in T47D and BT474 cells after 72 hours treatment of EO9. A-B) (A) *T47D* ***(B)*** *BT474 cells were treated with butylated hydroxytoluene (5000µM-0.00000001nM) and increasing concentrations of EO9 (100µM- 0.01nM) for 72 hours. Intracellular reactive oxygen species (ROS) levels were quantified using H_2DCFDA fluorescence assay. Fluorescence intensity was normalised to control and expressed as mean +/- SD.* ***C)*** *T47D and BT474 were treated with increasing concentrations of BHT (5000µM-0.00000001nM) under normoxic and hypoxic conditions for 72 hours. ID_{50} values were calculated based on dose response curves using a cell wizard*.

From figure 14 respective ID_{50} (ID_{50} refers to the concentration of BHT needed to inhibit a biological process by 50%) of BHT was used to treat the cell lines with EO9 for 72 hours before assessing cell viability (Figure 15). In normoxic conditions BT474 had increased sensitivity to inhibition of ROS with an ED_{50} of 1.3435 (+/- SD) compared to T47D which has a ED_{50} of 1.8049 (+/- SD) there is a non-significant increase in ED_{50} between the two cell lines. In hypoxic conditions T47D had increased sensitivity to inhibition of ROS with an ED_{50} of 1.63 (+/- SD). BT474 in hypoxic conditions which has a ED_{50} of 1.6455 (+/- SD) there is a non-significant increase in ED_{50} between the two cell lines. The cellular response to EO9 and BHT in combination was consistent between T47D and BT474 and there was no significant difference between ED_{50} in both cell lines.

A)

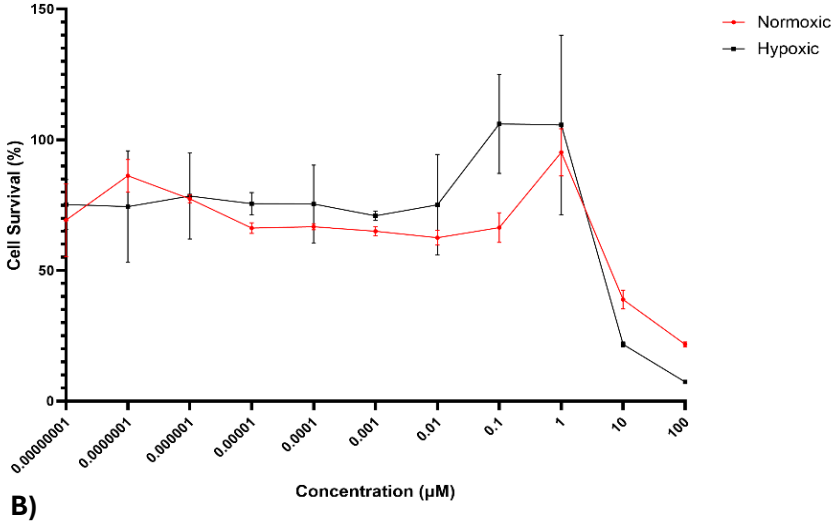

B)

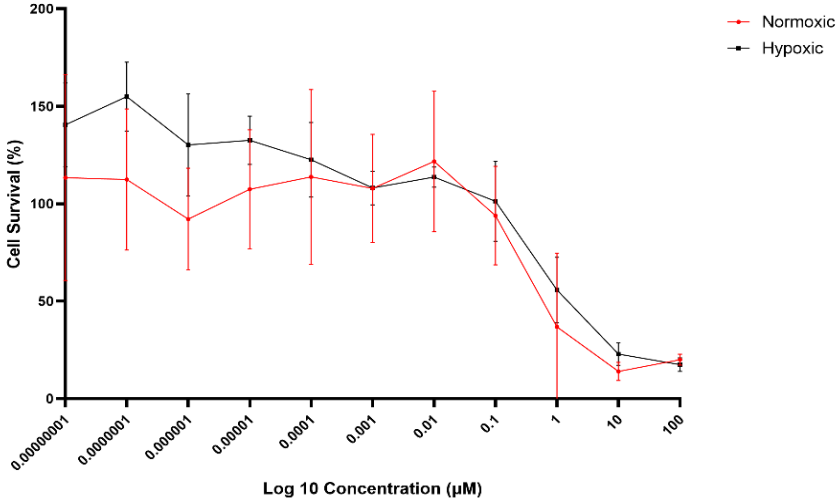

C)

	EO9		BHT	
	T47D (+/- SD) (µM)	**BT474 (+/- SD) (µM)**	**T47D (+/- SD)**	**BT474 (+/- SD)**
21% Oxygen	*0.02 (-/+0.01)*	*1.67 (-/+0.7)*	1.8049 (+/- 0.02)	1.3435 (+/- 0.072)
1% Oxygen	*0.0001 (-/+0.002)*	*0.016 (-/+0.05)*	1.6332 (+/- 0.142)	1.6455 (+/- 0.301)

Figure 15: The effect of ROS suppression on cell viability. A-B) (A) *T47D and* ***(B)*** *BT474 cells were treated with corresponding ID_{50} in hypoxic and normoxic conditions from figure 14C and increasing concentrations of EO9 (100μM- 0.01nM). Cell survival was quantified using an MTT assay and normalised to untreated controls and expressed +/- SD.* ***C)*** *T47D and BT474 were treated with corresponding ID_{50} of BHT and increasing concentrations of EO9 (100μM- 0.01nM) under normoxic and hypoxic conditions for 72 hours. ID_{50} values were calculated based on dose response curves using a cell wizard and shown in table.*

4.9 EO9 suppresses growth and integrity of Breast cancer Spheroids following prolonged exposure to EO9

Having shown the increased efficacy of EO9 in hypoxic 2D cell lines, the next step was to show whether EO9 penetrates 3D spheroids to gain access to the hypoxic core. To assess the long-term effects of EO9 on breast cancer spheroids, T47D and BT474 3D cultures were treated with EO9 (100μM - 1μM). Morphological changes were evaluated to determine EO9 impact on spheroids structure and to determine if EO9 was able to penetrate spheroid.

Post-treatment with EO9 the area of spheroid was evaluated by measuring the diameter of the spheroids. In untreated controls, both BT474 and T47D spheroids observed progressive growth with 474% and 65.79% increase in area respectively. Spheroids treated with 100μM-1μM saw a reduction in growth from day 1 to day 7 in both BT474 and T47D. The extent of this reduction was dose dependent with the most pronounced decrease observed at 100μM in were showing a 41.5% (BT474) and 53.6% (T47D) decrease in spheroid area. This effect was lost at 10μM where the spheroid area decreased by only 2% (BT474) and 1% (T47D) (Figure 16). At 1 μM BT474 cells decreased cell growth by 62% and T47D observed a decrease of 10% in spheroid area. These changes were consistent across all cell lines, indicating that EO9 is effective at disrupting spheroid integrity and supresses growth under prolonged exposure to EO9.

A)

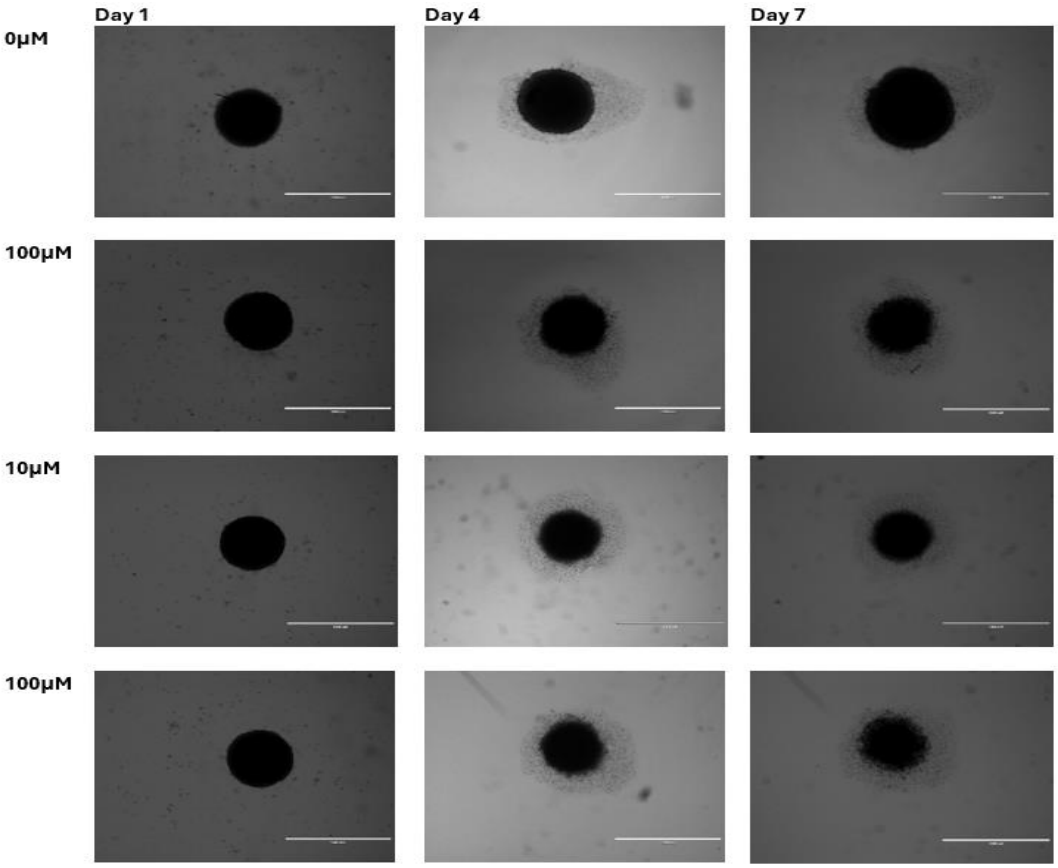
Day 1
Day 4
Day 7
0μM
100μM
10μM
100μM

C)

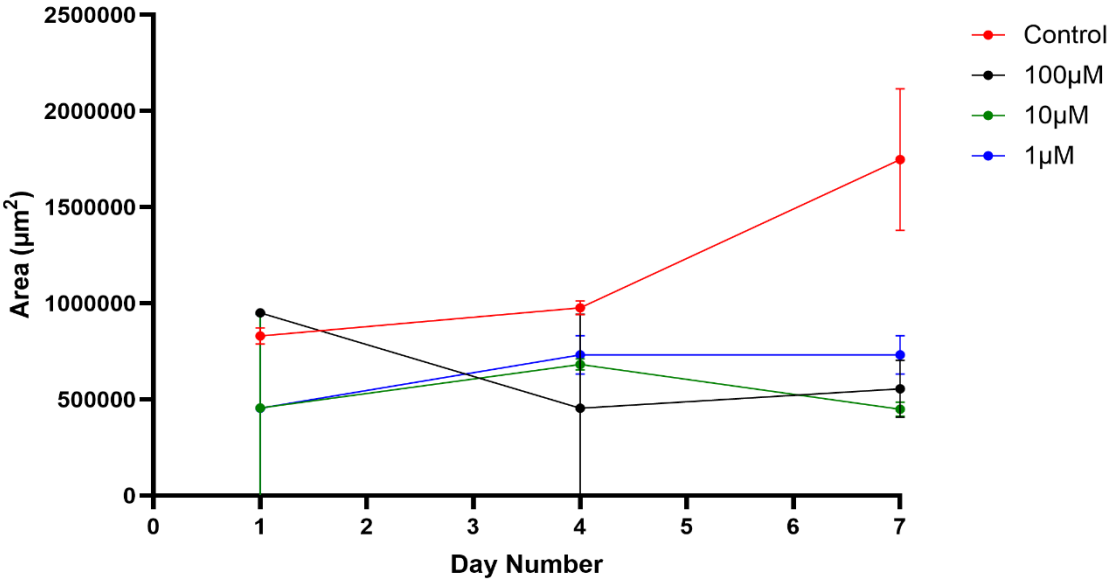
2500000
2000000
1500000
1000000
500000
0
Area (μm²)
0
1
2
3
4
5
6
7
Day Number
Control
100μM
10μM
1μM

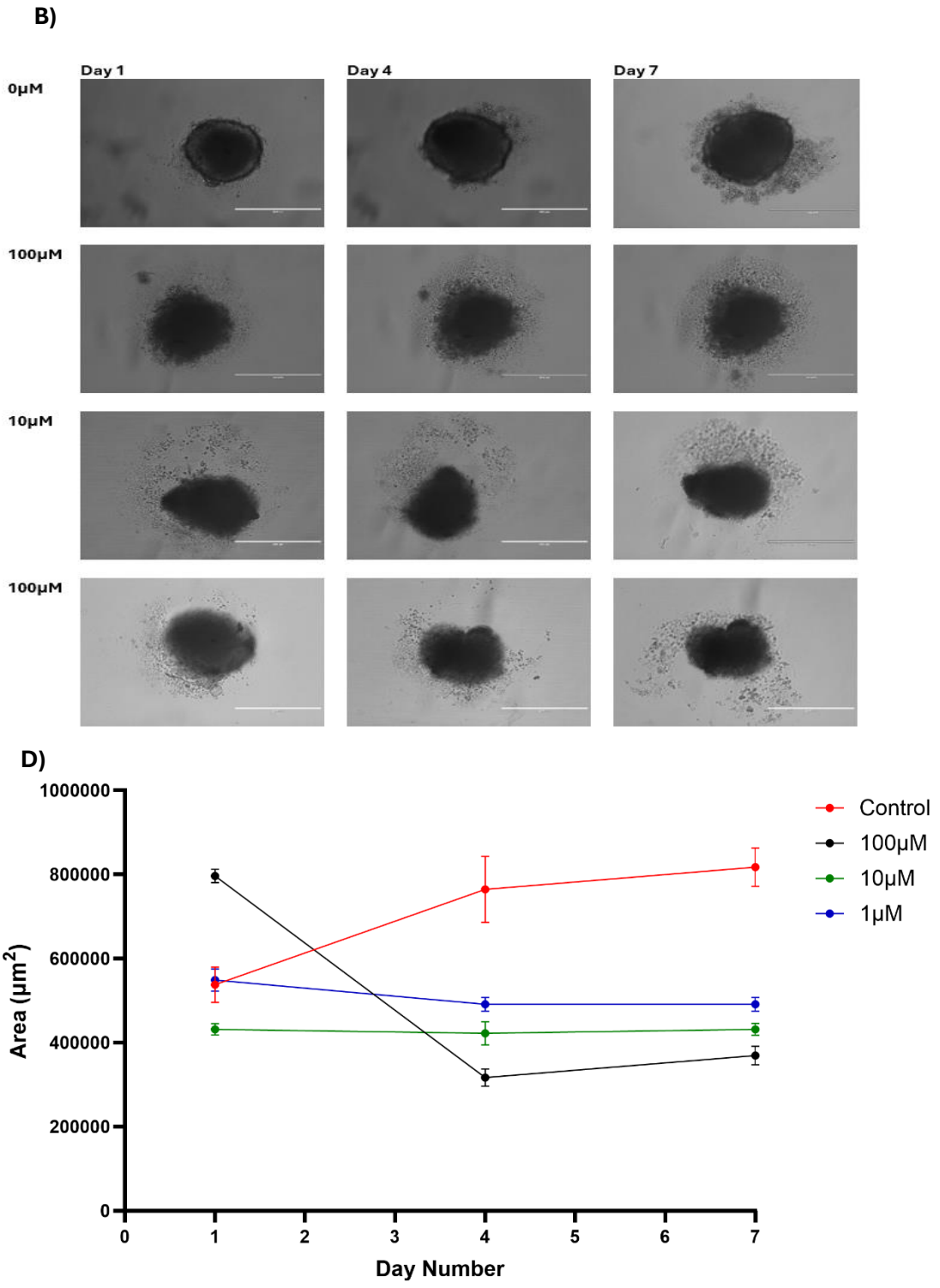

Figure 16. EO9 treatment reduces 3D spheroid growth of breast cancer cells over 7 days A-B) *Representative images of* ***(A)*** *BT474 spheroids* ***(B)*** *T47D seeded at 2x10^4 cells per well after 7 days of EO9 treatment at varying concentrations (100μM, 10μM, 1μM and 0μM) Scale bar = 1000μm.* ***C-D)*** *The mean spheroid area of* ***(C)*** *T47D* ***(D)*** *BT474 treated with EO9 at concentrations 100μM, 10μM, 1μM and 0μM measured on day 1, day 4 and day 7.*

5.0 Discussion

NQO1 is known to bioactivate EO9, a bio-reductive anti-cancer agent, although emerging evidence suggests that NQO1 activity alone does not consistently predict EO9 efficacy across breast cancer cell lines (Plumb, Gerritsen and Workman 1994; Phillips, R.M., Hendriks and Peters 2013). This discrepancy may be due to factors such as differential drug uptake, cellular redox status, or the presence of alternative metabolic pathways that influence EO9 activation or detoxification (Plumb, Gerritsen and Workman 1994; Puri et al. 2006; Phillips, R.M., Hendriks and Peters 2013).

Consequently, relying solely on NQO1 expression as a biomarker for EO9 sensitivity may lead to inaccurate therapeutic predictions. Therefore, further research is essential to unravel the complex interplay between NQO1 and EO9, identify additional determinants of drug response, and refine patient selection strategies to improve clinical outcomes.

5.1 Hypoxia induced modulation of EO9 activity

In both breast cancer cell lines evaluated, HIF-1α was upregulated which confirms a hypoxia response at a cellular level following exposure to 1% oxygen (Liu, L. et al. 2025) and may have implication for NQO1 expression. Although NQO1 is not a direct HIF-1α target (Tamaru et al. 2024), hypoxia-induced oxidative stress may activate the NRF2 pathways, indirectly increasing NQO1 levels. However, this response is context dependent and varies across tumour types and microenvironments (Choudry et al. 2001). To understand this relationship more precisely, NQO1 expression was normalised to β-actin, generating NQO1: β-actin ratios that provide a quantitative measure of relative protein abundance independent of loading variability. These ratios revealed that hypoxia does not uniformly induce NQO1 across breast cancer models. As, SiHa and T47D cells exhibited increased NQO1 expression under 1% oxygen, whereas BT474 cells demonstrated a higher NOQ1 expression under Normoxic conditions. This pattern indicates that NQO1 regulation is not soley governed by oxygen tension but is instead influenced by intrinsic cellular redox status, basal Nrf2 activity, and lineage-specific metabolic programming (Yang, L. et al. 2013; Ross and Siegel 2021).

EO9 cytotoxicity increased during hypoxia across cell lines, but this reflects a reduction in EO9 ED_{50} rather than a hypoxia induced change in NQO1 activity. In T47D cells, which exhibit low NQO1 activity (3.00 $x10^{-3}$ µmol/mg/min), the ED_{50} decreased under hypoxia, giving a hypoxic cytotoxicity ratio of 200.0. In BT474 cells, which have a higher NQO1

activity ($6.74x10^{-3}$ µmol/mg/min), ED_{50} also decreased under hypoxia, corresponding to a hypoxic cytotoxicity ratio of 104.38.

NQO1 plays a key role in EO9 cytotoxicity. For example, in breast cancer cell line MDA-MB-231 cells with low NQO1 activity (6 nmol/min 10^{-6}), a marked decrease in ID_{50} from 18,167 nM in normoxia to 24nM in hypoxia was reported, equating to a 700-fold decrease (Plumb and Workman 1994). In contrast, MCF7 cells with high NQO1 activity (4476 nmol/min 10^{-6} cells) showed only a 2-fold decrease in ID_{50} under hypoxia (Plumb and Workman 1994) suggesting NQO1 activity does not always correlate with EO9 efficacy. This supports the findings that EO9 activation may occur via alternative pathways. independent of NQO1 (Siegel, Reigan and Ross 2008; Phillips, R.M., Hendriks and Peters 2013).

Historically, low NQO1 expression limited EO9 efficacy, but hypoxia-driven 1-electron reduction may offer a therapeutic strategy for NQO1-deficent tumours (Chourdry et al. 2001). Semiquinones are more cytotoxic than hydroquinone due to their ROS generating redox cycling, leading to DNA fragmentation and caspase activation (Chouchane et al. 2006; Zhao et al. 2025). As such, NQO1 cannot be used reliably as a biomarker to predict EO9 treatment outcomes, as alternative activation pathways may drive EO9 efficacy, especially under hypoxic conditions.

EO9 treatment of T47D cells, which express low levels of NQO1, resulted in increased DNA damage under hypoxia, as shown by elevated γH2AX levels (figures 5 and 6). γH2AX is a well-established marker of DNA double strand breaks, forming rapidly at sites of damage, and therefore provides a marker of genotoxic stress. This pattern suggests that limited NQO1 activity restricts the usual 2-electron reduction of EO9 and instead favours the alternative 1-electron reduction pathway, generating semiquinone intermediates (Phillips, R.M. 2016). Semiquinones are unstable and readily produce reactive oxygen species (ROS), leading to oxidative stress, DNA damage, and ultimately cell death (Plumb and Workman 1994). Hypoxia further enhances ROS production through mitochondrial dysfunction and HIF-driven metabolic changes (Chandel et al. 1998). Together, these factors likely account for the heightened γH2AX signal observed in hypoxic T47D cells following EO9 exposure. So, this suggests the combination of a 1-electron reduction in the absence of NQO1 and amplification of ROS in hypoxic conditions leads to an increased DNA damaged which is indicated by elevated γH2AX levels (figures 5 and 6).

BT474 cells demonstrated a markedly different metabolic response to EO9 under hypoxia compared with T47D cells. In contrast to T47D, BT474 cells, which express higher levels of NQO1, showed reduced γH2AX levels under hypoxia, indicating less DNA damage. Increased NQO1 activity promotes efficient 2-electron reduction of EO9 to its hydroquinone

form, bypassing semiquinone formation and thereby minimising ROS generation (Plumb and Workman 1994). Consequently, the lower γH2AX signal in BT474 cells align with a more protective metabolic profile that limits EO9 induced oxidative DNA damage via generation of ROS.

5.2 Dissecting the role of NQO1 in hypoxia-driven EO9 activity

Measuring NQO1 protein expression levels alone can be misleading, as single nucleotide polymorphisms SNPs, like the common NQO1*2 polymorphism (C609T) can produce structurally unstable or functionally inactive variants (Lajin and Alachkar 2013). BT474 cells showed moderate NQO1 expression and activity under both normoxia and hypoxia. Western blot analysis revealed strong protein levels (24,377.5 DU), with enzymatic activity of $6.74x10^{-3}$ μmol/mg/min, confirming functional NQO1 (Table 3 and Figure 9). Immunofluorescence also indicated elevated NQO1 intensity compared to controls. Under hypoxia, staining intensity increased to 3.611 RFU, with a corresponding blot density of 13,980 DU, suggesting enhanced activation capacity and potential EO9 sensitivity.

Under hypoxic conditions, BT474 cells exhibited a marked increase in NQO1 staining intensity (3.611RFU) in hypoxia accompanied by a corresponding western blot densitometric value (13,980 DU), showing high NQO1 expression compared to negative control. These findings suggest that BT474 cells may possess an enhanced capacity to activate EO9 and mitigate oxidative stress, which could influence BT474 sensitivity to EO9 and drug metabolism.

T47D cells exhibited similar hypoxic responses. Under normoxia, fluorescence intensity was 1.9 RFU, with enzyme activity 3.00 $x10^{-3}$ μmol/mg/min, representing approximately 2-fold lower than BT474. Protein expression increased by 1.4-fold under hypoxia (from 13,980 DU to 19,896.6 DU), although fluorescence did not increase proportionally, possibly due to post-translational modifications (Salido et al. 2022). These findings suggest hypoxia-induced NQO1 upregulation may support oxidative stress resistance.

Other studies report variable NQO1 expression across breast cancer subtypes. Yang et al., (2014) found strong cytoplasmic staining in 61.9% of breast cancer cases, while MDA-MB-231 cells showed low activity (6 nmol/min 10^{-6} cells) (Plumb and Workman 1994), underscoring the need for context-specific analysis of EO9 responsiveness. A limitation of this study is that NOQ1 activity was assessed only under normoxia, leaving its hypoxic activity uncertain. While pancreatic cancer shows hypoxia-induced NQO1 upregulation, the mechanisms involved are not fully understood (Khan, A.E.M.A., Arutla and Srivenugopal 2024).NQO1 was once considered directly predictive of EO9 efficacy, although recent

findings show that EO9 remains effective in hypoxic conditions, with low NOQ1 levels suggesting alternative method of activation (Srijiwangsa and Na Bangchang 2017).

5.3 Dicumarol as a selective inhibitor of NQO1 and - impact on EO9 activation

A specific inhibitor of NQO1 was used to confirm the role of NQO1 activity in potentially driving the hypoxia-related increase in E09 activity. Dicumarol is a competitive inhibitor of NQO1, binding to its active site and preventing the 2-electron enzymatic reduction of EO9 to its active metabolite (Shaul et al. 2006). Dicumarol is considered a potent and specific NQO1 inhibitor with a low IC_{50}, with experimental studies showing that dicumarol has a low IC_{50} of 2.6nM in purified enzyme assays performed in the absence of serum proteins (Obi and Ezenwa 2018).

Under normal conditions, NQO1 mediated two electron reduction is the key bioactivation step that drives E09 induced cytotoxicity, so blocking this pathway should theoretically restore cell viability to approximately 100% (Choudry et al. 2001; Xiong et al. 2022). However, the experimental data demonstrate that viability remains substantially reduced even in the presence of dicumarol, indicating that EO9 continues to undergo metabolic activation through an alternative route. This indicates that, in the absence of NQO1, E09 is diverted into a one-electron reduction pathway, generating the semiquinone radical rather than the hydroquinone (Phillips, R.M., Hendriks and Peters 2013). The semiquinone readily undergoes redox cycling, producing superoxide and downstream ROS, thereby sustaining oxidative stress and preventing recovery of cell viability (Ho Yan 2005). The resulting oxidative stress is sufficient to maintain cytotoxicity independently of NOQ1 mediated activation. These findings demonstrate that EO9 possesses a dual activation mechanism, with the one electron semiquinone forming pathway capable of sustaining toxicity even when the two-electron reduction pathway is pharmacologically blocked (Phillips, R.M., Hendriks and Peters 2013). The mechanistic shift explains why dicumarol fails to rescue cell viability and highlights the importance of semiquinone driven redox cycling in determining the cellular response to EO9.

Co-treatment with dicumarol, resulted in an increase in EO9 induced cytotoxicity in both T47D and BT474. This was evidenced by a significant decrease of cell viability ($p < 0.01$) under Normoxic conditions, indicating that the inhibition of NQO1 impairs EO9 conversion to its active metabolite. With the inhibition of NQO1 this prevents the enzymatic 2-electron reduction to its hydroquinone and forces the 1-electron reduction of EO9 to semiquinone (Phillips, R.M., Hendriks and Peters 2013). Both BT474 and T47D express low to moderate levels of NQO1, and dicumarol treatment resulted in a measurable reduction in cytotoxicity, suggesting the involvement of NQO1 to some extent.

In normoxic conditions, both cell lines exhibited an increase in ROS production across all EO9 concentrations (Figure 12), indicating a strong pro-oxidant effect of EO9. Under hypoxia, the response was increased with certain concentrations showing a more marked ROS elevation, while others showed little to no changes. This suggests that oxygen tension influences EO9's redox activity, potentially through modulation of cellular metabolism or bio reductive activation pathways.

The addition of dicumarol, further amplified ROS generation in both cell lines. This enhancement was observed under both normoxic and hypoxic conditions, supporting the role of NQO1 in mitigating EO9 induced oxidative stress. Dicumarol alone did not exhibit direct cytotoxicity, but its co-treatment with EO9 significantly increased ROS levels ($P < 0.05$), implying that ROS generation causes EO9 cytotoxity in breast cancer cell lines.These findings highlight the interplay between EO9, oxygen availability, and NQO1 activity in regulating intracellular ROS. This suggests combining EO9 with NQO1 inhibitors like dicumarol may enhance therapeutic efficacy by promoting oxidative damage in cancer cells, particularly within hypoxic environments. Further investigation into downstream effects such as apoptosis, DNA damage and cell viability will be essential to fully understand the therapeutic potential of this combinatorial approach.

Although the findings show that dicumarol increases EO9 induced cytotoxicity, this outcome contrasts with the majority of published studies, which report that dicumarol reduces EO9 activity by inhibiting NQO1 dependent 2-electron reduction (Choudry et al. 2001; Phillips, R.M. 2016). This discrepancy is notable because EO9 is widely characterised as an NQO1 bioactivated agent, and inhibition of this pathway would typically be expected to reduce cytotoxic effects, rather than enhancing cytotoxic effects (Phillips, R.M., Hendriks and Peters 2013). However, EO9 is also capable of undergoing 1-electron reduction by alternative reductases such as cytochrome P450 reductase, particularly when NQO1 activity is limited (Bailey et al. 2001; Phillips, R.M., Hendriks and Peters 2013; Phillips, R.M. 2016). Cytochrome P450 reductase generate semiquinone radicals, which are unstable and prone to redox cycling, and thereby amplifying intracellular ROS (Bailey et al. 2001). In cell lines with modest NQO1 expression, such as T47D and BT474, this shift in metabolic balance may favour ROS driven toxicity rather than classical NQO1 mediated activation.

Both T47D and BT474 express low to moderate levels of NQO1, meaning that inhibition of the 2-electron reduction of EO9 may shift EO9 metabolism toward 1-electron reduction and semiquinone formation, thereby increasing ROS rather than supressing EO9 activation. Dicumarol has also been reported to exert off target effects, including mitochondrial uncoupling and redox cycling, which can independently elevate ROS and contribute to

cytotoxicity (Du et al. 2006). These off targets effects may amplify the impact of EO9 derived semiquinones, further intensifying oxidative stress in NQO1 deficient or moderately expressing cells. It is therefore likely that the enhanced cytotoxicity in hypoxia observed is due to multifactorial, which involves NQO1 inhibition and the off target effect of dicumarol.

Importantly, all dicumarol experiments in this study were performed under both Normoxic and hypoxic conditions, and in both environments dicumarol enhanced EO9 induced ROS generation. Given that hypoxia itself increases basal ROS through impaired mitochondrial electron transport, the combined effects of EO9 redox cycling, dicumarol induced ROS, and reduced NQO1 activity may create a highly oxidative intracellular environment that explains the enhanced cytotoxicity observed (Du et al. 2006; Phillips, R.M., Hendriks and Peters 2013; Phillips, R.M. 2016; Smith, Waypa and Schumacker 2017). This oxygen independent increase in ROS may account for the heightened cytotoxicity observed in the results despite the inhibitory effect of dicumarol on NQO1.

Although dicumarol inhibits NQO1 mediated bioactivation, the enhanced cytotoxicity observed in this study suggests that EO9's therapeutic potential may not solely on NQO1 dependent activation in low NQO1 tumours. Instead, dicumarol shifts EO9 metabolism toward 1-electron reduction and semiquinone formation, increasing ROS production (Nolan et al. 2010; Phillips, R.M. 2016; Obi and Ezenwa 2018). Importantly, tumours particularly in hypoxic regions which typically exhibit higher basal oxidative stress, impaired mitochondrial functional, and reduced antioxidant capacity compared with normal tissues (Smith, Waypa and Schumacker 2017). These vulnerabilities make cancer cells disproportionally sensitive to further ROS elevation. Normal cells, which generally maintain stronger redox buffering systems, are less likely to experience oxidative damage under the same conditions. Therefore, even though dicumarol reduces NQO1 activation of EO9, the resulting increase in ROS driven toxicity may still suggest a potential therapeutic advantage that warrants further investigation by selectively targeting tumour cells with compromised oxidative defences.

Dicumarol has promising use as an experimental tool in research due to its ability to inhibit NQO1, an enzyme which is responsible for the bioactivation of EO9. While its direct cytotoxicity remains a subject of concern, as treatment with dicumarol in breast cancer cell line (MCF-7) increased apoptosis (Aras et al. 2016). Although it is not understood whether this pro-apoptotic effect was due to the inhibition of NQO1 or direct cytotoxicity (Aras et al. 2016). These findings highlight the interaction between EO9, oxygen availability, and NQO1 activity in regulating intracellular ROS (Yang, L. et al. 2013; Ross and Siegel 2021). However, inhibiting NQO1 would be expected to reduce, rather than enhance, EO9 bioactivation, and this reduction would occur in both tumour and normal cells that express

NQO1 (Walton et al. 1992). Therefore, combining EO9 with NQO1 inhibitors such as dicumarol does not represent a strategy to improve therapeutic efficacy, but instead provides a mechanistic approach to determine the extent to which EO9 induced ROS and downstream effects depend on NQO1 activity. The combination of EO9 with NQO1 inhibitors is valuable for mechanistic studies rather than for enhancing therapeutic efficacy. Further investigation into downstream effects such as apoptosis, DNA damage and cell viability will be essential to fully understand the therapeutic potential of this combinatorial approach.

5.4 The impact of ROS inhibition on EO9-Induced Cytotoxicity

ROS inhibitors are widely used in research to help to deepen the understanding of ROS dependent pathway and are currently being explored therapeutically in conditions such as cancer (Glorieux et al. 2024). BHT is a synthetic antioxidant often used to inhibit ROS (IC_{50} 0.73μg/mL) (Maham 2024) and prevent oxidative damage and stress in biological systems (Dawidowicz and Olszowy 2011). The impact of BHT on EO9 treatment in T47D and BT474 breast cancer lines previously remains unexplored.

Treatment with BHT significantly ($p < 0.001$) increased the ED_{50} in normoxia and hypoxia in T47D but decreased the ED_{50} in BT474 under normoxia (by 0.33μM). However, in hypoxic a significant ($p<0.001$) increase in ED_{50} was noted (Figure 14). The decreased cytotoxicity observed in the presence of BHT upon EO9 treatment is likely due to BHT ability to scavenge ROS, which are a central part of EO9 activation (Dawidowicz and Olszowy 2011). When cells are BHT treated, ROS generation is inhibited before it can exert its cytotoxic effects, thereby protecting cells from oxidative stress (Dawidowicz and Olszowy 2011). This antioxidant interference reduces EO9 efficacy, especially in BT474 cells, possibly due to the higher expression of EO9 in BT474 cells leading to a higher ROS production (Phillips, R.M., Hendriks and Peters 2013). As a result, BHT acts as chemical shield preventing oxidative damage that EO9 relies on for activation to kill cancer cells.

ROS generation, possibly through semiquinone intermediates, was directly measured and found to correlate with increased cell death. This oxidative stress appears to play a significant role in the cytotoxic response, particularly in cells lacking NQO1 (Plumb, Gerritsen and Workman 1994). When ROS production was inhibited using BHT a marked increase in ED_{50} values was observed across all conditions, indicating reduced EO9 efficacy. These results highlight the contribution of ROS to activate EO9 independent of NQO1 and further emphasise that NQO1 expression alone does not account for treatment responsiveness to EO9.

BHT compared to other antioxidants such as BHA (IC_{50} approximatively 1.56µg/ml) and certain natural compounds like clove oil (IC_{50} approximatively 30µg/ml), demonstrated a superior radical quenching efficiency. BHT has dose dependent effects at low levels that are protective, whilst high levels can cause oxidative stress and trigger apoptosis in certain cell lines, such as murine fibroblasts and L929 fibrosarcoma cells (Liu et al., 2024).

5.5 EO9-induced cytotoxicity in 3D tumour spheroids

Unlike traditional 2D culture models, spheroids mimic the complex architecture of tumours, including nutrient gradients (Schaefer et al. n.d.; Zagaynova et al. 2017; Kirsh, Pascetta and Uniacke 2023). Although EO9 demonstrated potency in 2D, effectiveness in spheroids remains a challenge. Both cell lines (BT474 and T47D) expressed low to moderate levels of NQO1, which is believed to activate EO9 within spheroids (Chourdry et al. 2001). The inhibition of spheroid growth by EO9 indicates that EO9 is bioactivated to its active metabolite hydroquinone, leading to cell death and reducing spheroid growth (Workman 1994). As such, T47D and BT474 cells could serve as predictive model for EO9 responsiveness to solid breast cancer tumours and as a predictive model for breast tumours with a similar NQO1 expression.

Although EO9 penetration has not been directly measured within the spheroids, spheroid structure was disrupted, and growth reduced, as indicated by a halo of cells around the spheroids as EO9 penetrates across multicellular layers of cells due to its small molecular size (315.28 g/mol) (Phillips, R.M., Hendriks and Peters 2013). This penetration across multiple layers of cells may offer therapeutic benefit, as tumours are composed of numerous densely packed cell layers, which contributes to tumours reduced accessibility and makes tumours difficult to treat. Although EO9 is capable of penetrating multicellular layers, EO9 rate of penetration is comparatively slow relative to other therapeutics. This limitation should be recognised when interpreting EO9 performance in multicellular tumour models, as reduced penetration may constrain EO9's overall effectiveness in densely structured tumour tissues (Phillips, R.M., Loadman and Cronin 1998).

Although this study was partially conducted in spheroid models, a notable limitation is that hypoxia within the spheroid cores was not directly measured during EO9 treatment. Given that spheroids naturally develop oxygen gradients, meaning that a hypoxic core often naturally form (Kirsh, Pascetta and Uniacke 2023). All spheroids used in treatment with EO9 met the hypoxic threshold of a diameter of 150µm and so it was presumed that all spheroids had hypoxic cores present (Kirsh, Pascetta and Uniacke 2023).

Previous studies have shown a major contrast between EO9 efficacy in monolayer cell culture compared to spheroids. While EO9 demonstrates potent activity in colon adenocarcinoma monolayer cell cultures (ID_{50} =0.76µg/ml), this potency significantly decreased in spheroid growth conditions (Bibby, Cronin and Phillips, R.M. 1993), which may suggest that the hypoxic core of spheroids, alongside NQO1 expression, may not be enough for EO9 activation. Alternatively,, EO9 drug penetration may be limited due to the microenvironment created by 3D cell cultures.

5.6 Future Works

EO9 faces significant delivery challenges that limit its clinical success. When administered systemically, it is rapidly metabolised by cytochrome P450 reductase which is present in red blood cells and inactivates it before reaching its target (Puri et al. 2006) thus limiting its use in breast cancer. To address this, EO9 can be delivered by intravesical instillation into the bladder, though its efficacy depends on timing and post-surgical conditions (Puri et al. 2006).

Implantable drug delivery devices offer a promising solution by enabling localised, substantiated EO9 release at the tumour site, bypassing systemic inactivation and enhancing efficacy (Puri et al. 2006). Technologies like biodegradable implants, drug-eluting stent, and micro-reservoir pumps have been used to improve precision, reduce dosing frequency and minimise toxicity (Puri et al. 2006; Villarruel Mendoza et al. 2020; Gupta, Sarkar and Saha 2023; Lungu, Creteanu and Mehedinti 2024).

Despite NOQ1 being a key enzyme in EO9 activation, relying solely on its expression may overlook broader redox influences. EO9 requires a reductive environment, and other biomarkers such as glutathione peroxidase and superoxide dismutase may better reflect cellular conditions for activation (Carmo de Carvalho e Martins et al. 2022). Elevated malondialdehyde levels, indicating oxidative stress, which may also further enhance EO9 cytotoxicity.

5.7 Conclusion

Although NQO1 plays a central role in the bioactivation of EO9, NQO1 expression is highly variable across tumour types and can fluctuate in response to microenvironmental and treatment related factors (Hua et al. 2021; Weng et al. 2021; Tamaru et al. 2024). Although NQO1 expression varies across tumour types, this variability may also be advantageous, as it allows EO9 to be selectively targeted to patients whose tumours express NQO1, thereby supporting more individualised therapeutic strategies. However, despite this potential advantage, the variability in NQO1 expression is unpredictable and highly context dependent, meaning it cannot reliably indicate which tumours will respond to EO9.

This observation further supports the conclusion that NOQ1 is not a reliable marker of responsiveness. Despite T47D exhibiting lower NQO1 expression and activity than BT474 cells, T47D demonstrated greater cytotoxicity under hypoxic conditions. This inverse relationship highlights the need for more robust and consistent biomarkers and so relying solely on NQO1 expression could result in misleading predictions in therapeutic contexts.

The findings outlined in this report demonstrate that NQO1 expression is not a reliable marker of EO9 treatment responsiveness. Despite its variable activity across cell lines, cytotoxicity was more closely related to ROS generation via semiquinone intermediates, especially under hypoxic conditions. The enhanced cell death in T47D cell, the effects of NQO1 inhibition with dicumarol, and the increased ED_{50} upon ROS suppression with BHT all point to oxidative stress as a key driver of EO9 sensitivity and so therapeutic predictions should consider boarder redox dynamics, rather than relying solely on NQO1 levels.

Bibliography:

Ahmad, A., Wu, Y. and Yang, W. (2013) Pathways to Breast Cancer Recurrence. *International Scholarly Research Notices* [Post-print], 2013 (1), p. 290568. Available from https://onlinelibrary.wiley.com/doi/full/10.1155/2013/290568. [Accessed 26th July 2024].

Aras, D., Cinar, O., Cakar, Z., Ozkavukcu, S. and Can, A. (2016) Can dicoumarol be used as a gonad-safe anticancer agent: an in vitro and in vivo experimental study. *Molecular Human Reproduction* [Post-print], 22 (1), pp. 57–67. Available from https://dx.doi.org/10.1093/molehr/gav065. [Accessed 16th October 2025].

Bailey, S.M., Lewis, A.D., Patterson, L.H., Fisher, G.R., Knox, R.J. and Workman, P. (2001) Involvement of NADPH: Cytochrome P450 reductase in the activation of indoloquinone EO9 to free radical and DNA damaging species. *Biochemical Pharmacology* [Post-print], 62 (4), pp. 461–468. Available from https://pubmed-ncbi-nlm-nih-gov.yorksj.idm.oclc.org/11448456/. [Accessed 10th May 2026].

Basheeruddin, M. and Qausain, S. (2024) Hypoxia-Inducible Factor 1-Alpha (HIF-1α) and Cancer: Mechanisms of Tumor Hypoxia and Therapeutic Targeting. *Cureus* [Post-print], 16 (10), p. e70700. Available from https://pmc.ncbi.nlm.nih.gov/articles/PMC11529905/. [Accessed 16th October 2025].

Bhattacharya, A., Alam, K., Roy, N.S., Kaur, K., Kaity, S., Ravichandiran, V. and Roy, S. (2023) Exploring the interaction between extracellular matrix components in a 3D organoid disease model to replicate the pathophysiology of breast cancer. *Journal of Experimental and Clinical Cancer Research* [Post-print], 42 (1), pp. 1–29. Available from https://jeccr.biomedcentral.com/articles/10.1186/s13046-023-02926-4. [Accessed 1st October 2025].

Bhutta, B.S., Alghoula, F. and Berim, I. (2024) Hypoxia. *StatPearls* [Internet], Available from https://www.ncbi.nlm.nih.gov/books/NBK482316/. [Accessed 16th October 2025].

Białkowska, K., Komorowski, P., Bryszewska, M. and Miłowska, K. (2020) Spheroids as a Type of Three-Dimensional Cell Cultures—Examples of Methods of Preparation and the Most Important Application. *International Journal of Molecular Sciences* [Post-print], 21 (17), p. 6225. Available from https://pmc.ncbi.nlm.nih.gov/articles/PMC7503223/. [Accessed 28th October 2025].

Bibby, M.C., Cronin, B.P. and Phillips, R.M. (1993) Evaluation of the cytotoxicity of the indoloquinone EO9 in a human colon adenocarcinoma model. *International Journal of Oncology* [Post-print], 3 (4), pp. 661–666. Available from http://www.spandidos-publications.com/10.3892/ijo.3.4.661/abstract. [Accessed 1st October 2025].

Carmo de Carvalho e Martins, M. do, da Silva Santos Oliveira, A.S., da Silva, L.A.A., Primo, M.G.S. and de Carvalho Lira, V.B. (2022) Biological Indicators of Oxidative Stress [Malondialdehyde, Catalase, Glutathione Peroxidase, and Superoxide Dismutase] and Their Application in Nutrition. pp. 833–856. Available from https://link.springer.com/rwe/10.1007/978-3-031-07389-2_49. [Accessed 9th October 2025].

Chandel, N.S., Maltepe, E., Goldwasser, E., Mathieu, C.E., Simon, M.C. and Schumacker, P.T. (1998) Mitochondrial reactive oxygen species trigger hypoxia-induced transcription. *Proceedings of the National Academy of Sciences* [Post-print], 95 (20), pp. 11715–11720. Available from /doi/pdf/10.1073/pnas.95.20.11715?download=true. [Accessed 16th October 2025].

Chen, Y. and Gaber, T. (2021) Hypoxia/HIF Modulates Immune Responses. *Biomedicines 2021, Vol. 9, Page 260* [Post-print], 9 (3), p. 260. Available from https://www.mdpi.com/2227-9059/9/3/260/htm. [Accessed 16th October 2025].

Cheng, L., Yu, H., Yan, N., Lai, K. and Xiang, M. (2017) Hypoxia-inducible factor-1α target genes contribute to retinal neuroprotection. *Frontiers in Cellular Neuroscience* [Post-print], 11, p. 218972. Available from www.frontiersin.org. [Accessed 24th October 2025].

Chouchane, S., Wooten, J.B., Tewes, F.J., Wittig, A., Müller, B.P., Veltel, D. and Diekmann, J. (2006) Involvement of semiquinone radicals in the in vitro cytotoxicity of cigarette mainstream smoke. *Chemical research in toxicology* [Post-print], 19 (12), pp. 1602–1610. Available from https://pubmed-ncbi-nlm-nih-gov.yorksj.idm.oclc.org/17173373/. [Accessed 23rd October 2025].

Choudry, G.A., Stewart, P.A.H., Double, J.A., Krul, M.R.L., Naylor, B., Flannigan, G.M., Shah, T.K., Brown, J.E. and Phillips, R.M. (2001) A novel strategy for NQO1 (NAD(P)H:quinone oxidoreductase, EC 1.6.99.2) mediated therapy of bladder cancer based on the pharmacological properties of EO9. *British Journal of Cancer* [Post-print], 85 (8), pp. 1137–1146. Available from http://hdl.handle.net/10454/3889. [Accessed 30th September 2025].

Chourdry, G., Stewart, H.P., Double, J., Kurl, M., Naylor, B., Flannigan, G., Shah, T., Brown, J. and Phillips, R. (2001) A novel strategy for NQO1 (NAD(P)H:quinone oxidoreductase, EC 1.6.99.2) mediated therapy of bladder cancer based on the pharmacological properties of EO9. *British Journal of cancer* [Internet], Available from http://www.bjcancer.com. [Accessed 1st October 2025].

Chua, Y.L., Dufour, E., Dassa, E.P., Rustin, P., Jacobs, H.T., Taylor, C.T. and Hagen, T. (2010) Stabilization of hypoxia-inducible factor-1α protein in hypoxia occurs independently of mitochondrial reactive oxygen species production. *Journal of Biological Chemistry* [Post-print], 285 (41), pp. 31277–31284. Available from https://www.jbc.org/action/showFullText?pii=S0021925819888610. [Accessed 5th April 2026].

Darby, S., McGale, P., Correa, C., Taylor, C., Arriagada, R., Clarke, M., Cutter, D., Davies, C., Ewertz, M., Godwin, J., Gray, R., Pierce, L., Whelan, T., Wang, Y., Peto, R., Albain, K., Anderson, S., Barlow, W., Bergh, J., Bliss, J., Buyse, M., Cameron, D., Carrasco, E., Coates, A., Collins, R., Costantino, J., Cuzick, J., Davidson, N., Davies, K., Delmestri, A., Di Leo, A., Dowsett, M., Elphinstone, P., Evans, V., Gelber, R., Gettins, L., Geyer, C., Goldhirsch, A., Gregory, C., Hayes, D., Hill, C., Ingle, J., Jakesz, R., James, S., Kaufmann, M., Kerr, A., MacKinnon, E., McHugh, T., Norton, L., Ohashi, Y., Paik, S., Pan, H.C., Perez, E., Piccart, M., Pritchard, K., Pruneri, G., Raina, V., Ravdin, P., Robertson, J., Rutgers, E., F Shao, Y., Swain, S., Valagussa, P., Viale, G., Winer, E. and Wood, W. (2011) Effect of radiotherapy after breast-conserving surgery on 10-year recurrence and 15-year breast cancer death: meta-analysis of individual patient data for 10 801 women in 17 randomised trials. *The Lancet*, 378 (9804), pp. 1707–1716.

Dassarma, B., Mahapatra, S.K., Nandi, D.K., Gangopadhyay, S. and Samanta, S. (2025) Protective role of butylated hydroxyanisole (BHA) and hydroxytoluene (BHT) against oxidative stress-induced inflammatory response in carbon tetrachloride-induced acute hepatorenal toxicity. *Archives of Physiology and Biochemistry* [Post-print], 131 (5), pp. 728–735. Available from https://www-tandfonline-com.yorksj.idm.oclc.org/doi/pdf/10.1080/13813455.2025.2493105. [Accessed 28th October 2025].

Dawidowicz, A.L. and Olszowy, M. (2011) Antioxidant properties of BHT estimated by ABTS assay in systems differing in pH or metal ion or water concentration. *European Food Research and Technology* [Post-print], 232 (5), pp. 837–842. Available from https://link.springer.com/article/10.1007/s00217-011-1451-7. [Accessed 7th October 2025].

Dong, H., Hao, L. and Zhou, Z. (2021) AhR-NQO1 Signaling in Hepatocytes Drives a Protective Response against Alcohol-induced NAD+ Depletion and Liver Damage. *Recent Developments in Medicine and Medical Research Vol. 16* [Post-print], pp. 43–67. Available from https://stm.bookpi.org/RDMMR-V16/article/view/5240. [Accessed 6th October 2025].

Douda, D.N., Khan, M.A., Grasemann, H. and Palaniyar, N. (2015) SK3 channel and mitochondrial ROS mediate NADPH oxidase-independent NETosis induced by calcium influx. *Proceedings of the National Academy of Sciences of the United States of America* [Post-print], 112 (9), pp. 2817–2822. Available from https://www.pnas.org/doi/pdf/10.1073/pnas.1414055112. [Accessed 7th October 2025].

Du, J., Daniels, D.H., Asbury, C., Venkataraman, S., Liu, J., Spitz, D.R., Oberley, L.W. and Cullen, J.J. (2006) Mitochondrial Production of Reactive Oxygen Species Mediate Dicumarol-induced Cytotoxicity in Cancer Cells. *Journal of Biological Chemistry* [Post-print], 281 (49), pp. 37416–37426. Available from https://www.sciencedirect.com/science/article/pii/S0021925820719150. [Accessed 10th May 2026].

Faraji, P., Borchert, A., Ahmadian, S. and Kuhn, H. (2024) Butylated Hydroxytoluene (BHT) Protects SH-SY5Y Neuroblastoma Cells from Ferroptotic Cell Death: Insights from In Vitro and In Vivo Studies. *Antioxidants* [Post-print], 13 (2), p. 242. Available from https://www.mdpi.com/2076-3921/13/2/242/htm. [Accessed 8th October 2025].

Garcia-Llorens, G., El Ouardi, M. and Valls-Belles, V. (2025) Oxidative Stress Fundamentals: Unraveling the Pathophysiological Role of Redox Imbalance in Non-Communicable Diseases. *Applied Sciences 2025, Vol. 15, Page 10191* [Post-print], 15 (18), p. 10191. Available from https://www.mdpi.com/2076-3417/15/18/10191/htm. [Accessed 8th October 2025].

Glorieux, C., Liu, S., Trachootham, D. and Huang, P. (2024) Targeting ROS in cancer: rationale and strategies. *Nature Reviews Drug Discovery 2024 23:8* [Post-print], 23 (8), pp. 583–606. Available from https://www.nature.com/articles/s41573-024-00979-4. [Accessed 8th October 2025].

Gupta, N., Sarkar, C. and Saha, S. (2023) Biodegradable Polymers—Carriers for Drug Delivery. *Materials Horizons: From Nature to Nanomaterials* [Post-print], Part F1245, pp. 149–168. Available from https://link.springer.com/chapter/10.1007/978-981-99-3307-5_7. [Accessed 9th October 2025].

Hayes, J.D., Dinkova-Kostova, A.T. and Tew, K.D. (2020) Oxidative Stress in Cancer. *Cancer Cell* [Post-print], 38 (2), pp. 167–197. Available from https://www.cell.com/action/showFullText?pii=S1535610820302749. [Accessed 8th October 2025].

Ho Yan, Y. (2005) Effect of Superoxide Anion and Hydrogen Peroxide on Ca^^ Mobilization in Microvascular Endothelial Cells: A Possible Role of TRPM2.

Hompland, T., Fjeldbo, C.S. and Lyng, H. (2021) Tumor Hypoxia as a Barrier in Cancer Therapy: Why Levels Matter. *Cancers 2021, Vol. 13, Page 499* [Post-print], 13 (3), p. 499. Available from https://www.mdpi.com/2072-6694/13/3/499/htm. [Accessed 16th October 2025].

Hu, Y., Shen, M., Wang, C., Huang, Q., Li, R., Dorj, G., Gombojav, E., Du, J. and Ren, L. (2024) A meta-analysis-based adverse outcome pathway for the male reproductive toxicity induced by microplastics and nanoplastics in mammals. *Journal of Hazardous Materials* [Post-print], 465. Available from https://pubmed-ncbi-nlm-nih-gov.yorksj.idm.oclc.org/38160553/. [Accessed 7th October 2025].

Hua, H.S., Li, L., Hui, W., Li, Z., Ji, D., Yun, P.R., Hong, Z., Hua, H.S., Li, L., Hui, W., Li, Z., Ji, D., Yun, P.R. and Hong, Z. (2021) Activation of Nrf2/NQO1 Pathway Attenuates Oxidative Stress in Neuronal Cells

Induced by Microwave and Protects Neurite Development. *Biomedical and Environmental Sciences, 2021, Vol. 34, Issue 11, Pages: 931-936* [Post-print], 34 (11), pp. 931–936. Available from https://www.besjournal.com/en/article/doi/10.3967/bes2021.129. [Accessed 6th October 2025].

Huppertz, B. (2023) Placental physioxia is based on spatial and temporal variations of placental oxygenation throughout pregnancy. *Journal of Reproductive Immunology*, 158.

Ježek, J., Cooper, K.F. and Strich, R. (2018) Reactive Oxygen Species and Mitochondrial Dynamics: The Yin and Yang of Mitochondrial Dysfunction and Cancer Progression. *Antioxidants 2018, Vol. 7, Page 13* [Post-print], 7 (1), p. 13. Available from https://www.mdpi.com/2076-3921/7/1/13/htm. [Accessed 8th October 2025].

Johansson, E., Parkinson, G.N., Denny, W.A. and Neidle, S. (2003) Studies on the nitroreductase prodrug-activating system. Crystal structures of complexes with the inhibitor dicoumarol and dinitrobenzamide prodrugs and of the enzyme active form. *Journal of medicinal chemistry* [Post-print], 46 (19), pp. 4009–4020. Available from https://pubmed-ncbi-nlm-nih-gov.yorksj.idm.oclc.org/12954054/. [Accessed 16th October 2025].

Kahl, R. (1992) Butylated Hydroxytoluene Toxicity. *Lipid-Soluble Antioxidants: Biochemistry and Clinical Applications* [Post-print], pp. 590–605. Available from https://link.springer.com/chapter/10.1007/978-3-0348-7432-8_47. [Accessed 29th October 2025].

Kasai, S., Shimizu, S., Tatara, Y., Mimura, J. and Itoh, K. (2020) Regulation of Nrf2 by Mitochondrial Reactive Oxygen Species in Physiology and Pathology. *Biomolecules 2020, Vol. 10, Page 320* [Post-print], 10 (2), p. 320. Available from https://www.mdpi.com/2218-273X/10/2/320/htm. [Accessed 8th October 2025].

Khan, A.E.M.A., Arutla, V. and Srivenugopal, K.S. (2024) Human NQO1 as a Selective Target for Anticancer Therapeutics and Tumor Imaging. *Cells 2024, Vol. 13, Page 1272* [Post-print], 13 (15), p. 1272. Available from https://www.mdpi.com/2073-4409/13/15/1272/htm. [Accessed 30th September 2025].

Kirsh, S.M., Pascetta, S.A. and Uniacke, J. (2023) Spheroids as a 3D Model of the Hypoxic Tumor Microenvironment. *Methods in Molecular Biology* [Post-print], 2614, pp. 273–285. Available from https://link.springer.com/protocol/10.1007/978-1-0716-2914-7_17. [Accessed 3rd October 2025].

Lajin, B. and Alachkar, A. (2013) The NQO1 polymorphism C609T (Pro187Ser) and cancer susceptibility: a comprehensive meta-analysis. *British Journal of Cancer* [Post-print], 109 (5), p. 1325. Available from https://pmc.ncbi.nlm.nih.gov/articles/PMC3778271/. [Accessed 23rd October 2025].

Liu, L., Yu, J., Liu, Y., Xie, L., Hu, F. and Liu, H. (2025) Hypoxia-driven angiogenesis and metabolic reprogramming in vascular tumors. *Frontiers in Cell and Developmental Biology* [Post-print], 13, p. 1572909. Available from https://pmc.ncbi.nlm.nih.gov/articles/PMC12119610/. [Accessed 16th October 2025].

Liu, S., Tang, C., Jiang, K., Zhang, L., Ma, N., Li, Y., Fan, M. and Huang, B. (2024) Toxicity of energetic nanomaterials assessed on L929 fibroblasts. *Chemical Papers* [Post-print], 78 (6), pp. 3507–3514. Available from https://link.springer.com/article/10.1007/s11696-024-03324-6. [Accessed 8th October 2025].

Lungu, C.N., Creteanu, A. and Mehedinti, M.C. (2024) Endovascular Drug Delivery. *Life 2024, Vol. 14, Page 451* [Post-print], 14 (4), p. 451. Available from https://www.mdpi.com/2075-1729/14/4/451/htm. [Accessed 9th October 2025].

Ma, Y., Kong, J., Yan, G., Ren, X., Jin, D., Jin, T., Lin, L. and Lin, Z. (2014) NQO1 overexpression is associated with poor prognosis in squamous cell carcinoma of the uterine cervix. *BMC Cancer* [Post-print], 14 (1), p. 414. Available from https://pmc.ncbi.nlm.nih.gov/articles/PMC4058702/. [Accessed 27th October 2025].

Maham, F. (2024) Identification and comparison of antioxidant, antibacterial and physico-chemical properties of different essential oils | Monthly Hamqadam. Available from https://hamqadam.com.pk/en/node/123. [Accessed 8th October 2025].

Mutter, F.E., Park, B.K. and Copple, I.M. (2015) Value of monitoring Nrf2 activity for the detection of chemical and oxidative stress. *Biochemical Society Transactions*, 43 (4), pp. 657–662.

Nolan, K.A., Scott, K.A., Barnes, J., Doncaster, J., Whitehead, R.C. and Stratford, I.J. (2010) Pharmacological inhibitors of NAD(P)H quinone oxidoreductase, NQO1: Structure/activity relationships and functional activity in tumour cells. *Biochemical Pharmacology* [Post-print], 80 (7), pp. 977–981. Available from https://www.sciencedirect.com/science/article/abs/pii/S0006295210004582. [Accessed 16th October 2025].

Obi, J.C. and Ezenwa, T.E. (2018) Synthesis of Analogues of Dicoumarol and their Biological Evaluation.. Julie C Obi et al Synthesis of Analogues of Dicoumarol and their Biological Evaluation. *Singaporean Journal of Scientific Research(SJSR) An International Journal (AMIJ* [Post-print], 10 (1), pp. 1–9. Available from www.sjsronline.com. [Accessed 8th October 2025].

Pant, A., Dasgupta, D., Tripathi, A. and Pyaram, K. (2023) Beyond Antioxidation: Keap1–Nrf2 in the Development and Effector Functions of Adaptive Immune Cells. *ImmunoHorizons* [Post-print], 7 (4), pp. 288–298. Available from https://dx.doi.org/10.4049/immunohorizons.2200061. [Accessed 6th October 2025].

Patiño-Morales, C.C., Soto-Reyes, E., Arechaga-Ocampo, E., Ortiz-Sánchez, E., Antonio-Véjar, V., Pedraza-Chaverri, J. and García-Carrancá, A. (2019) Curcumin stabilizes p53 by interaction with NAD(P)H:quinone oxidoreductase 1 in tumor-derived cell lines. *Redox Biology* [Post-print], 28, p. 101320. Available from https://pmc.ncbi.nlm.nih.gov/articles/PMC6807312/. [Accessed 27th October 2025].

Pedersen, R.N., Mellemkjær, L., Ejlertsen, B., Nørgaard, M. and Cronin-Fenton, D.P. (2022) Mortality After Late Breast Cancer Recurrence in Denmark. *Journal of Clinical Oncology* [Post-print], 40 (13), pp. 1450–1463. Available from https://ascopubs.org/doi/10.1200/JCO.21.02062. [Accessed 26th July 2024].

Phillips, R.M. (2016) Targeting the hypoxic fraction of tumours using hypoxia-activated prodrugs. *Cancer Chemotherapy and Pharmacology*, 77 (3), pp. 441–457.

Phillips, R.M., Hendriks, H.R. and Peters, G.J. (2013) EO9 (Apaziquone): from the clinic to the laboratory and back again. *British Journal of Pharmacology*, 168 (1), pp. 11–18.

Phillips, R.M., Loadman, P.M. and Cronin, B.P. (1998) Evaluation of a novel in vitro assay for assessing drug penetration into avascular regions of tumours. *British Journal of Cancer* [Post-print], 77 (12), pp. 2112–2119. Available from https://www.ncbi.nlm.nih.gov/pmc/articles/PMC2150429. [Accessed 6th October 2025].

Phillips, R.M., Wheelhouse, R., Flannigan, G.M., Shah, T., Puri, R., Basu, S., Mirejovsky, D., Lenaz, G., Gill, J.H. and Abdallah, Q.M. (2006) Analysis of NAD(P)H:quinone oxidoreductase-1 (NQO1),

Cytochrome P450 Oxidoreductase (P450R) and Glucose transporter 1 (Glut-1) protein expression suggests a possible role for EO9 in the treatment of invasive bladder cancer. *American Association Cancer Reasearch*, 6 (8).

Piwocka, O., Sterzyńska, K., Malińska, A., Suchorska, W.M. and Kulcenty, K. (2025) Development of tetraculture spheroids as a versatile 3D model for personalized breast cancer research. Available from www.nature.com/scientificreports. [Accessed 1st October 2025].

Plumb, J.A., Gerritsen, M. and Workman, P. (1994) DT-diaphorase protects cells from the hypoxic cytotoxicity of indoloquinone EO9. *British Journal of Cancer 1994 70:6* [Post-print], 70 (6), pp. 1136–1143. Available from https://www.nature.com/articles/bjc1994461. [Accessed 23rd October 2024].

Plumb, J.A. and Workman, P. (1994) Unusually marked hypoxic sensitization to indoloquinone EO9 and mitomycin C in a human colon-tumour cell line that lacks DT-diaphorase activity. *International journal of cancer* [Post-print], 56 (1), pp. 134–139. Available from https://pubmed-ncbi-nlm-nih-gov.yorksj.idm.oclc.org/8262670/. [Accessed 6th October 2025].

Puri, R., Palit, V., Loadman, P.M., Flannigan, M., Shah, T., Choudry, G.A., Basu, S., Double, J.A., Lenaz, G., Chawla, S., Beer, M., Van Kalken, C., de Boer, R., Beijnen, J.H., Twelves, C.J. and Phillips, R.M. (2006) Phase I/II Pilot Study of Intravesical Apaziquone (EO9) for Superficial Bladder Cancer. *The Journal of Urology* [Post-print], 176 (4), pp. 1344–1348. Available from /doi/pdf/10.1016/j.juro.2006.06.047. [Accessed 7th October 2025].

Ross, D. and Siegel, D. (2021) The diverse functionality of NQO1 and its roles in redox control. *Redox Biology* [Post-print], 41, p. 101950. Available from https://pmc.ncbi.nlm.nih.gov/articles/PMC8027776/. [Accessed 10th May 2026].

Salido, E., Timson, D.J., Betancor-Fernández, I., Palomino-Morales, R., Anoz-Carbonell, E., Pacheco-García, J.L., Medina, M. and Pey, A.L. (2022) Targeting HIF-1α Function in Cancer through the Chaperone Action of NQO1: Implications of Genetic Diversity of NQO1. *Journal of Personalized Medicine 2022, Vol. 12, Page 747* [Post-print], 12 (5), p. 747. Available from https://www.mdpi.com/2075-4426/12/5/747/htm. [Accessed 31st October 2025].

Samuel, J. and Franklin, C. (2008) Hypoxemia and Hypoxia. *Common Surgical Diseases* [Post-print], pp. 391–394. Available from https://link.springer.com/chapter/10.1007/978-0-387-75246-4_97. [Accessed 24th October 2025].

Schaefer, W., Hedemann N, Christmann T, Guledani A, Sebens S, Geisen R and Pirsch, & (n.d.) Detection of Necrotic Cores in Tumor Spheroids Using a Live/Dead Assay and NYONE ® Scientific IMAGE AND EVALUATE MORE SPHEROIDS IN LESS TIME. Available from www.synentec.com. [Accessed 6th October 2025].

Shaikat, A.H., Azad, S.M.A.K., Tamim, Md.A.R., Ullah, M.S., Amin, M.N., Sabbir, M.K., Tarun, M.T.I., Mostaq, M.S., Sabrin, S., Mahmud, M.Z. and Mahmud, M.A. (2025) Investigating hypoxia-inducible factor signaling in cancer: mechanisms, clinical implications, targeted therapeutic strategies, and resistance. *Cancer Pathogenesis and Therapy* [Internet], Available from https://www.sciencedirect.com/science/article/pii/S2949713225000904. [Accessed 16th October 2025].

Shaul, Y., Asher, G., Dym, O., Tsvetkov, P. and Adler, J. (2006) Crystal Structure of NQO1 with Dicoumarol. *Worldwide Protein Data Bank* [Internet], Available from https://www.wwpdb.org/pdb?id=pdb_00002f1o. [Accessed 1st October 2025].

Shen, J., Rasmussen, M., Dong, Q.R., Tepel, M. and Scholze, A. (2017) Expression of the NRF2 Target Gene NQO1 Is Enhanced in Mononuclear Cells in Human Chronic Kidney Disease. *Oxidative Medicine and Cellular Longevity* [Post-print], 2017 (1), p. 9091879. Available from https://onlinelibrary.wiley.com/doi/pdf/10.1155/2017/9091879. [Accessed 6th October 2025].

Siegel, D., Reigan, P. and Ross, D. (2008) One- and Two-Electron-Mediated Reduction of Quinones: Enzymology and Toxicological Implications. *Advances in Bioactivation Research* [Post-print], pp. 1–29. Available from https://link.springer.com/chapter/10.1007/978-0-387-77300-1_7. [Accessed 6th October 2025].

Smith, K.A., Waypa, G.B. and Schumacker, P.T. (2017) Redox signaling during hypoxia in mammalian cells. *Redox Biology* [Post-print], 13, pp. 228–234. Available from https://www.sciencedirect.com/science/article/pii/S2213231717302355. [Accessed 10th May 2026].

Son, Y., Cheong, Y.-K., Kim, N.-H., Chung, H.-T., Kang, D.G. and Pae, H.-O. (2011) Mitogen-Activated Protein Kinases and Reactive Oxygen Species: How Can ROS Activate MAPK Pathways? *Journal of Signal Transduction* [Post-print], 2011 (1), p. 792639. Available from /doi/pdf/10.1155/2011/792639. [Accessed 8th October 2025].

Srijiwangsa, P. and Na Bangchang, K. (2017) Roles of NAD (P) H-Quinone Oxidoreductase 1 (NQO1) On Cancer Progression and Chemoresistance. *Journal of Clinical & Experimental Oncology*, 06 (04).

Swinney, D.C. (2011) Molecular Mechanism of Action (MMoA) in Drug Discovery. *Annual Reports in Medicinal Chemistry* [Post-print], 46, pp. 301–317. Available from https://www.sciencedirect.com/science/chapter/bookseries/abs/pii/B9780123860095000096. [Accessed 25th June 2026].

Tamaru, E., Kokubu, D., Ushida, Y. and Itoh, K. (2024) Nrf2 induction potency of plant-derived compounds determined using an antioxidant response element luciferase reporter and conventional NAD(P)H-quinone acceptor oxidoreductase 1 activity assay. *BMC Research Notes* [Post-print], 17 (1), pp. 1–7. Available from https://bmcresnotes.biomedcentral.com/articles/10.1186/s13104-024-07038-6. [Accessed 30th September 2025].

Villarruel Mendoza, L.A., Scilletta, N.A., Bellino, M.G., Desimone, M.F. and Catalano, P.N. (2020) Recent Advances in Micro-Electro-Mechanical Devices for Controlled Drug Release Applications. *Frontiers in Bioengineering and Biotechnology*, 8, p. 556016.

Walton, M.I., Bibby, M.C., Double, J.A., Plumb, J.A. and Workman, P. (1992) DT-diaphorase activity correlates with sensitivity to the indoloquinone EO9 in mouse and human colon carcinomas. *European Journal of Cancer* [Post-print], 28 (10), pp. 1597–1600. Available from https://www.ejcancer.com/action/showFullText?pii=0959804992900498. [Accessed 10th May 2026].

Weng, B., Zhang, X., Chu, X., Gong, X. and Cai, C. (2021) Nrf2-Keap1-ARE-NQO1 signaling attenuates hyperoxia-induced lung cell injury by inhibiting apoptosis. *Molecular Medicine Reports* [Post-print], 23 (3), pp. 1–1. Available from http://www.spandidos-publications.com/10.3892/mmr.2021.11860/abstract. [Accessed 6th October 2025].

Workman, P. (1994) Enzyme-directed bioreductive drug development revisited: a commentary on recent progress and future prospects with emphasis on quinone anticancer agents and quinone metabolizing enzymes, particularly DT-diaphorase. *Oncology research*, 6 (10–11), pp. 461–75.

Xiong, Y., Kaw, H.Y., Zhu, L. and Wang, W. (2022) Genotoxicity of quinone: An insight on DNA adducts and its LC-MS-based detection. *Critical Reviews in Environmental Science and Technology* [Post-print],

52 (23), pp. 4217–4240. Available from https://www.tandfonline.com/doi/abs/10.1080/10643389.2021.2001276. [Accessed 24th October 2025].

Yang, L., Zahid, M., Liao, Y., Rogan, E.G., Cavalieri, E.L., Davidson, N.E., Yager, J.D., Visvanathan, K., Groopman, J.D. and Kensler, T.W. (2013) Reduced formation of depurinating estrogen–DNA adducts by sulforaphane or KEAP1 disruption in human mammary epithelial MCF-10A cells. *Carcinogenesis* [Post-print], 34 (11), p. 2587. Available from https://pmc.ncbi.nlm.nih.gov/articles/PMC3888356/. [Accessed 10th May 2026].

Yang, Y., Zhang, Y., Wu, Q., Cui, X., Lin, Z., Liu, S. and Chen, L. (2014) Clinical implications of high NQO1 expression in breast cancers. *Journal of Experimental and Clinical Cancer Research* [Post-print], 33 (1), pp. 1–9. Available from https://link.springer.com/articles/10.1186/1756-9966-33-14. [Accessed 16th October 2025].

Yuhan, L., Khaleghi Ghadiri, M. and Gorji, A. (2024) Impact of NQO1 dysregulation in CNS disorders. *Journal of Translational Medicine* [Post-print], 22 (1), pp. 1–28. Available from https://translational-medicine.biomedcentral.com/articles/10.1186/s12967-023-04802-3. [Accessed 30th September 2025].

Zagaynova, E. V., Druzhkova, I.N., Mishina, N.M., Ignatova, N.I., Dudenkova, V. V. and Shirmanova, M. V. (2017) Imaging of Intracellular pH in Tumor Spheroids Using Genetically Encoded Sensor SypHer2. *Advances in Experimental Medicine and Biology* [Post-print], 1035, pp. 105–119. Available from https://link.springer.com/chapter/10.1007/978-3-319-67358-5_7. [Accessed 6th October 2025].

Zhao, H.Q., Yu, R., Liu, J., Cheng, H., Ding, A., Zhang, D., Mu, Y. and Lu, P. (2025) Quinone structure regulates sulfide-driven reactive oxygen species generation for aquatic pollutant degradation. *Water Research* [Post-print], 288, p. 124571. Available from https://www.sciencedirect.com/science/article/abs/pii/S0043135425014757. [Accessed 23rd October 2025].

Zhou, J., Lan, F., Liu, M., Wang, F., Ning, X., Yang, H. and Sun, H. (2024) Hypoxia inducible factor-1α as a potential therapeutic target for osteosarcoma metastasis. *Frontiers in Pharmacology*, 15, p. 1350187.

6. Supplementary data

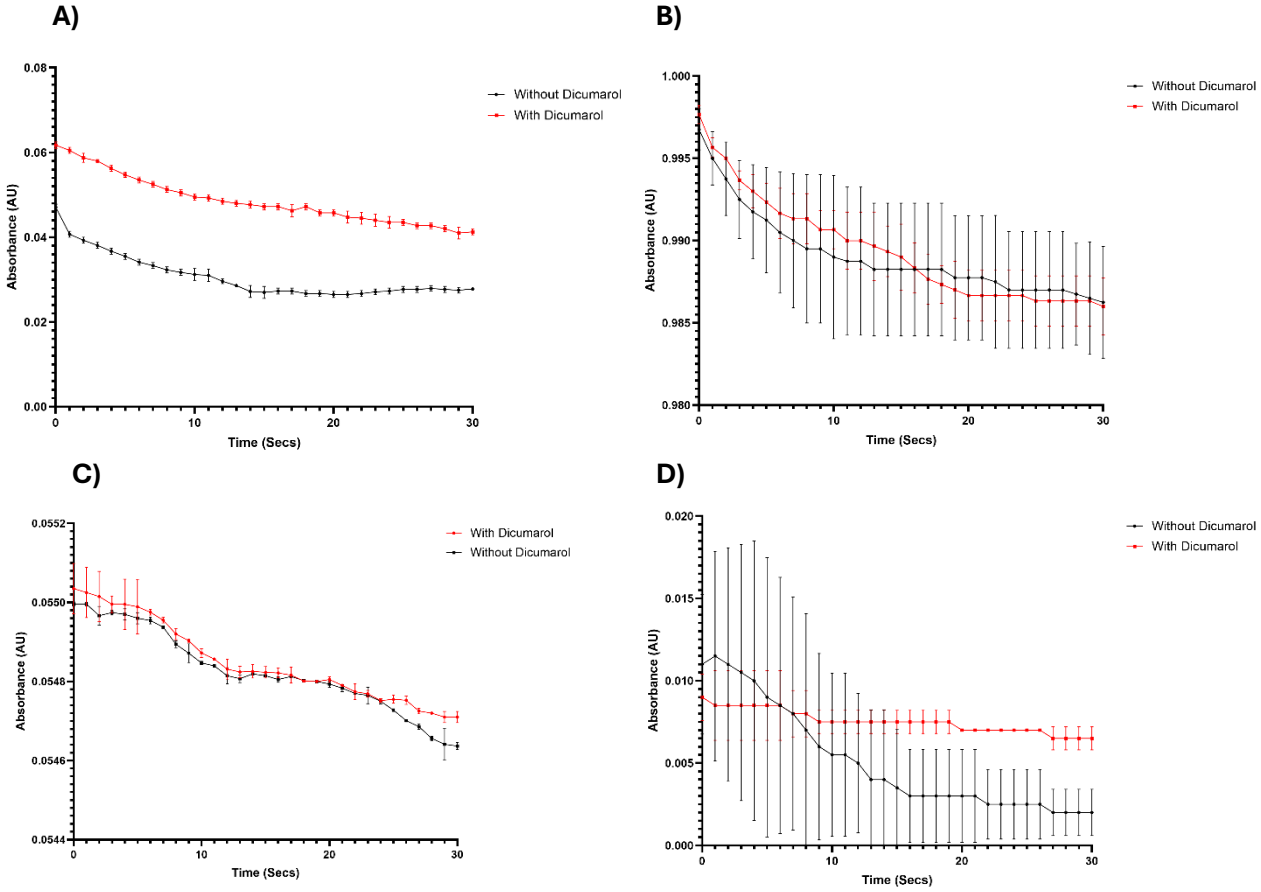

Figure 17: Dicumarol sensitive NQO1 activity assessed by DCPIP reduction: A) *BT474* ***B)*** *T47D* ***C)*** *CaSki* ***D)****SiHa NQO1 activity levels assessed by the spectrophotometric reduction of DCPIP in the presence and absence of dicumarol.*